








# Autophagy receptor ZmNBR1 promotes the autophagic degradation of ZmBRI1a and enhances drought tolerance in maize

Yang Xiang<sup>1,2†</sup> , Guangdong Li<sup>1†</sup> , Qian Li<sup>1</sup> , Yingxue Niu<sup>1</sup> , Yitian Pan<sup>1</sup> , Yuan Cheng<sup>1</sup> , Xiangli Bian<sup>1</sup> , Chongyang Zhao<sup>1</sup> , Yuanhong Wang<sup>1</sup>  and Aying Zhang<sup>1,2,3\*</sup> 

1. College of Life Sciences, Nanjing Agricultural University, Nanjing 210095, China

2. State Key Laboratory of Crop Genetics & Germplasm Enhancement and Utilization, Nanjing Agricultural University, Nanjing 210095, China

3. Sanya Institute of Nanjing Agricultural University, Nanjing Agricultural University, Sanya 572025, China

<sup>†</sup>These authors contributed equally to this work.

\*Correspondence: Aying Zhang ([ayzhang@njau.edu.cn](mailto:ayzhang@njau.edu.cn))



Yang Xiang



Aying Zhang

## ABSTRACT

Drought stress is a crucial environmental factor that limits plant growth, development, and productivity. Autophagy of misfolded proteins can help alleviate the damage caused in plants experiencing drought. However, the mechanism of autophagy-mediated drought tolerance in plants remains largely unknown. Here, we cloned the gene for a maize (*Zea mays*) selective autophagy receptor, *NEXT TO BRCA1 GENE 1* (*ZmNBR1*), and identified its role in the response to drought stress. We observed that drought stress increased the accumulation of autophagosomes. RNA sequencing and reverse transcription-quantitative polymerase chain reaction showed that *ZmNBR1* is markedly induced by drought stress. *ZmNBR1* overexpression enhanced drought

tolerance, while its knockdown reduced drought tolerance in maize. Our results established that *ZmNBR1* mediates the increase in autophagosomes and autophagic activity under drought stress. *ZmNBR1* also affects the expression of genes related to autophagy under drought stress. Moreover, we determined that BRASSINOSTEROID INSENSITIVE 1A (*ZmBRI1a*), a brassinosteroid receptor of the BRI1-like family, interacts with *ZmNBR1*. Phenotype analysis showed that *ZmBRI1a* negatively regulates drought tolerance in maize, and genetic analysis indicated that *ZmNBR1* acts upstream of *ZmBRI1a* in regulating drought tolerance. Furthermore, *ZmNBR1* facilitates the autophagic degradation of *ZmBRI1a* under drought stress. Taken together, our results reveal that *ZmNBR1* regulates the expression of autophagy-related genes, thereby increasing autophagic activity and promoting the autophagic degradation of *ZmBRI1a* under drought stress, thus enhancing drought tolerance in maize. These findings provide new insights into the autophagy degradation of brassinosteroid signaling components by the autophagy receptor *NBR1* under drought stress.

Keywords: autophagy receptor, drought tolerance, *Zea mays*, *ZmBRI1a*, *ZmNBR1*

Xiang, Y., Li, G., Li, Q., Niu, Y., Pan, Y., Cheng, Y., Bian, X., Zhao, C., Wang, Y., and Zhang, A. (2024). Autophagy receptor *ZmNBR1* promotes the autophagic degradation of *ZmBRI1a* and enhances drought tolerance in maize. *J. Integr. Plant Biol.* **66**: 1068–1086.

## INTRODUCTION

Drought stress severely affects plant growth, development, and productivity (Kuromori et al., 2022; Zhang et al., 2022a). When subjected to drought stress, plants sense and

transmit signals that alter cell metabolism and initiate various protective mechanisms. Many factors, including receptor proteins, protein kinases, transcription factors, and metabolic enzymes, function in drought tolerance (Todaka et al., 2015; Xiang et al., 2021a; Zhang et al., 2022a). Despite the progress

in identifying these factors, the detailed mechanisms of plant drought tolerance remain to be elucidated. Understanding these mechanisms is necessary to improve crop drought tolerance and ensure sustainable agricultural production in a changing climate (Siddiqui et al., 2021; Zhang et al., 2022a).

Autophagy is an evolutionarily conserved macromolecular degradation process that maintains intracellular metabolic homeostasis by sending damaged proteins into the vacuole for degradation in plants (Suttangkakul et al., 2011; Li et al., 2020). Autophagy is closely related to seed development, pollen germination, leaf senescence, and stress responses (Wang et al., 2015; Zhao et al., 2020; Paluch-Lubawa et al., 2021; Qi et al., 2021; Wei et al., 2021; Yu and Hua, 2022). Drought stress causes the accumulation of misfolded proteins that damage the cell membrane systems and organelles, and even induce plant cell death (Sun et al., 2018; Jia et al., 2021). Some factors have been reported to regulate the autophagic process in response to drought stress. For instance, the heat shock transcription factor HsfA1a directly activates the expression of *autophagy-related 10* (ATG10) and *ATG18f* to induce autophagy to degrade drought-induced insoluble proteins and enhance drought tolerance in tomato (*Solanum lycopersicum*) (Wang et al., 2015). The dehydrin cold acclimation-specific 31 (MtCAS31) interacts with ATG8 to promote autophagic degradation of plasma membrane intrinsic protein 2;7 (MtPIP2;7), a negative regulator of drought tolerance, to improve drought tolerance in *Medicago truncatula* (Li et al., 2020). Plant-specific *constitutively stressed 1* (COST1) reduces drought tolerance by repressing autophagy in plants (Bao et al., 2020). Nevertheless, the mechanism of autophagy-mediated drought tolerance in plants is poorly understood.

The autophagy receptor Next to BRCA1 gene 1 (NBR1) was first identified in mammals. The NBR1 proteins are structurally conserved; they all contain a PB1 domain, a ZZ-type zinc finger domain, and a NBR1/FW domain as well as two ubiquitin-binding domains, UBA domains, in their C termini (Su et al., 2021; Zhang et al., 2022b). NBR1 proteins recognize specific substrates and feed them into the selective autophagy pathway (Zhou et al., 2013; Thirumalaikumar et al., 2021; Zhang et al., 2022b). When selective autophagy begins, NBR1 is rapidly accumulated, and its C-terminal UBA1 and UBA2 domains interact with ubiquitin-modified proteins. The NBR1/FW domain of NBR1 binds to ATG8 to form a protein complex. Other ATG proteins assist in the formation of autophagosomes. The autophagosomes then wrap around protein aggregates and subsequently transfer them to the vacuole for degradation and recycling (Lamark et al., 2009; Jung et al., 2020; Zhang and Chen, 2020). NBR1 has an essential role in plant growth, development, and stress responses (Hafren et al., 2017; Su et al., 2021; Thirumalaikumar et al., 2021). Loss-of-function mutants of *NBR1* in Arabidopsis (*Arabidopsis thaliana*) exhibit an early-senescence phenotype under short-day conditions and an increased number of lateral root initiation sites, while *AtNBR1*-overexpressing plants show delayed germination and increased numbers of closed stomata

(Ji et al., 2020; Tarnowski et al., 2020). *Nicotiana benthamiana* Joka2/NBR1 contributes to the defense against *Phytophthora infestans* (Dagdas et al., 2016), suggesting that NBR1 is also involved in plant immunity. NBR1 also plays a critical role in abiotic stress. For instance, tomato *NBR1a* and *NBR1b* and poplar *NBR1* improve cold and salt stress tolerance (Chi et al., 2020; Su et al., 2021). Arabidopsis plants heterologously expressing the wheat (*Triticum aestivum*) *NBR1*-like gene showed enhanced drought sensitivity (Chen et al., 2022). Furthermore, AtNBR1 interacts with its autophagy substrates Heat shock protein 90.1 (HSP90.1) and rotamase FKBP 1 (ROF1) and facilitates their autophagic degradation during heat stress recovery (Thirumalaikumar et al., 2021). However, it is not clear whether NBR1 and its specific autophagy substrates are involved in autophagic degradation in response to drought stress.

Here, we identified the function of the maize (*Zea mays*) autophagy receptor ZmNBR1 in drought stress and found that Brassinosteroid insensitive 1a (ZmBRI1a), a brassinosteroid (BR) receptor of the BRI1-like family, interacts with ZmNBR1. We demonstrated that ZmNBR1 regulates the expression of genes related to autophagy to improve autophagic activity, and promotes the autophagic degradation of ZmBRI1a, thus enhancing drought tolerance in maize.

## RESULTS

### Drought stress increases the accumulation of autophagosomes and up-regulates ZmNBR1 expression

We performed monodansylcadaverine (MDC) staining to detect autophagosomes in maize leaf cells under drought stress. When maize plants were exposed to drought stress, maize leaf cells had considerably more autophagosomes than they did under normal conditions (Figure 1A). The autophagic activity was 4.5-fold higher in plants treated with drought stress for 2 d compared with plants grown in normal conditions. The activity increased to a maximum value (14.6-fold) at 6 d of drought treatment (Figure 1B). Next, we detected the ratio of ZmATG8a-PE/ZmATG8a, which was closely related to autophagy activity, and the protein level of ZmATG13a, a marker for autophagy, in maize leaves under drought stress. The ZmATG8a-PE/ZmATG8a ratio began to increase at 2 d of drought treatment and peaked at 6 d (Figure 1C, E). Similarly, the protein level of ZmATG13a began to increase at 2 d of drought treatment and peaked at 6 d (Figure 1D, F). These results show that drought stress increases the accumulation of autophagosomes and the relative autophagic activity.

To further clarify the function of autophagy in drought stress, we conducted RNA sequencing (RNA-seq) using three-leaf-stage maize seedlings treated with drought for 4 d in three independent experiments. We first performed a heat map of correlation analysis between the samples. The correlation coefficients between all biological replicates were

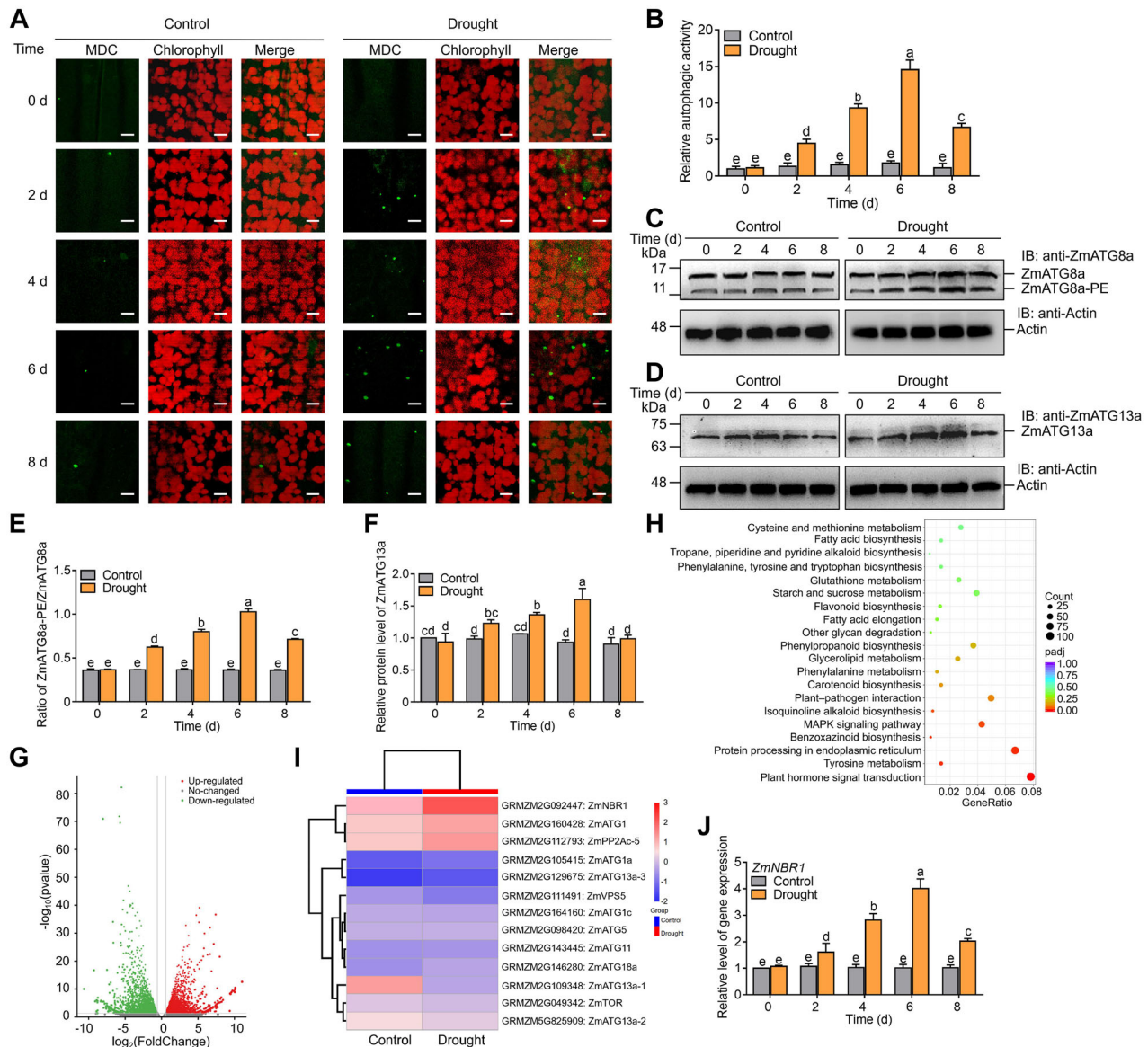


**Figure 1. Drought induces the accumulation of autophagosomes and up-regulates *ZmNBR1* expression in maize**

(A) Monodansylcadaverine (MDC)-stained autophagosomes (green fluorescence). Maize plants at the three-leaf stage were treated with drought stress for 8 d. Autophagosomes were stained by MDC (50  $\mu\text{mol/L}$ ) in the second leaves. Scale bars, 10  $\mu\text{m}$ . (B) Relative autophagic activity under drought stress shown in (A). The number of autophagosomes divided by the total number of mesophyll cells represented the relative autophagic activity. (C) The ratio of ZmATG8a-PE/ZmATG8a and (D) the protein level of ZmATG13a in maize leaves under drought stress. The proteins were detected with anti-ZmATG8a and anti-ZmATG13a antibodies. ZmActin was used as the loading control. (E) Statistical analysis of the ratio of ZmATG8a-PE/ZmATG8a and (F) ZmATG13a protein level shown in (C) and (D). The control at 0 d was set to 1. (G) Volcano plots representing the fold change of differentially expressed genes (DEGs) under drought stress. Gray dots represent genes without significant changes in expression. (H) Kyoto Encyclopedia of Genes and Genomes (KEGG) pathway enrichment analysis showing the top 20 enriched terms for clustered DEGs. The bubble chart shows the enriched terms. (I) Expression heatmap showing the genes closely associated with the autophagic process. (J) Expression of *ZmNBR1* under drought stress. Maize plants at the three-leaf stage were treated with drought stress, and expression was analyzed in the second leaves. The values of the control at 0 d were set as 1. *ZmActin* was used as the internal reference. Data are means ( $\pm\text{SD}$ ) of three biological replicates. Different letters indicate significant differences at  $P < 0.05$  according to two-way analysis of variance (Tukey's multiple comparison tests).

greater than 0.8 and verified the repeatability among the replicates (Figure S1). Differentially expressed genes (DEGs) were identified with the set criteria of  $|\log_2 \text{Fold Change}| > 1$  and  $P < 0.05$ . We identified 6,744 DEGs between the drought-stressed and control plants, among which 3,112 (46.14%) genes were up-regulated and 3,632 (53.86%) genes were down-regulated (Figure 1G). Kyoto Encyclopedia of

Genes and Genomes (KEGG) pathway enrichment for the DEGs showed that plant hormone signal transduction, amino acid metabolism, sugar metabolism, and the mitogen-activated protein kinase (MAPK) pathway were involved in the drought stress response (Figure 1H). Based on the results of comparative and functional analysis of the DEGs, we selected genes closely associated with the autophagic process



for an expression heatmap. The heatmap showed that *ZmNBR1*, encoding a maize selective autophagy receptor, was significantly induced by drought stress (Figure 1I). Furthermore, to verify if drought affects the expression of *ZmNBR1*, we detected its expression by reverse transcription-quantitative polymerase chain reaction (RT-qPCR) under drought stress compared with the control condition. *ZmNBR1* expression increased at 2 d of drought treatment, peaked at 6 d, and was increased compared to the control at 8 d (Figure 1J). These results suggest that *ZmNBR1* may be involved in the drought stress response.

### Molecular characterization of ZmNBR1

The 2,529-bp full-length complementary DNA (cDNA) sequence of *ZmNBR1* encodes a polypeptide of 842 amino acid residues. Multiple sequence alignment analysis showed that the ZmNBR1 protein contains an N-terminal PB1 domain, a ZZ-type zinc finger domain, a NBR1/Four Tryptophan (FW) domain, and two C-terminal UBA domains (UBA1 and UBA2) (Figure 2A). The phylogenetic tree showed that ZmNBR1 and sorghum (*Sorghum bicolor*) SbNBR1 proteins have the closest genetic relationship and share 88.32% similarity. ZmNBR1 shared 79.50%, 36.76%, 37.42%,

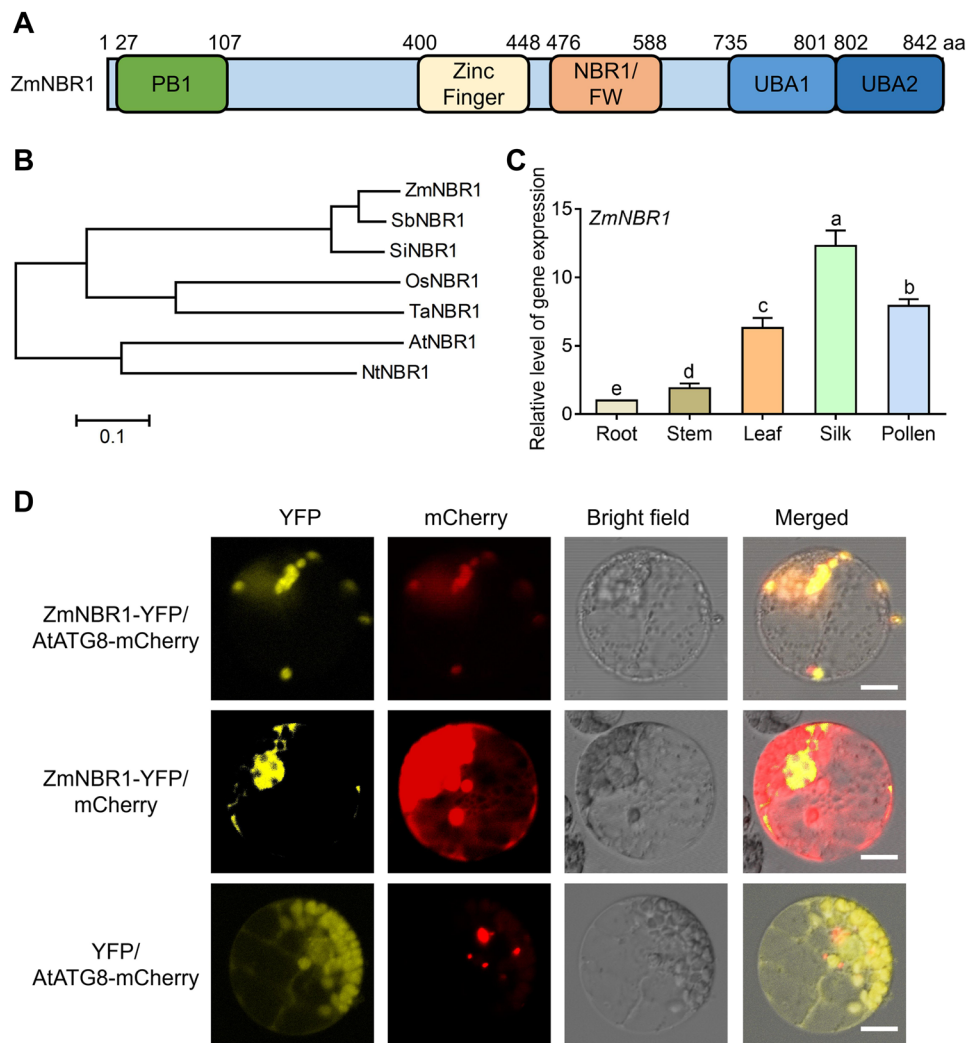


**Figure 2. Molecular characterization and subcellular localization of ZmNBR1**

(A) *ZmNBR1* encodes a protein of 842 amino acid residues and contains an N-terminal Phox and Bem1 (PB1) domain, a NBR1/Four Tryptophan (FW) domain, and two C-terminal Ubiquitin-Associated (UBA) domains. (B) Phylogenetic tree of NBR1 proteins drawn using MEGA software (version 5.0). The phylogenetic relationship between the protein sequences was assessed using the neighbor-joining method with *p*-distance correction. Bootstrap values were derived from 1,000 replicate runs. NBR1 protein sequences were derived from *Zea mays*, *Sorghum bicolor*, *Setaria italica*, *Oryza sativa*, *Triticum aestivum*, *Arabidopsis thaliana*, and *Nicotiana tabacum* and included ZmNBR1 (GRMZM2G092447), SbNBR1 (XP\_002454107), SiNBR1 (XP\_004952961), OsNBR1 (XP\_015625351), TaNBR1 (QEE80346), AtNBR1 (NP\_194200), and NtNBR1 (XP\_016458014). (C) Expression of *ZmNBR1* in different maize tissues. Root, stem, and leaf samples were taken from plants at the three-leaf stage, whereas silk and pollen samples were taken from plants at the flowering stage. *ZmActin* was used as the internal reference. *ZmUbi:ZmNBR1-YFP* and *ZmUbi:YFP* constructs were separately transfected into maize protoplasts. *ZmUbi:AtATG8-mCherry* was used as a marker for autophagosome localization. Scale bars, 10 μm. Data are means (±SD) of three biological replicates. Different letters indicate significant differences at *P* < 0.05 according to two-way analysis of variance (Tukey's multiple comparison tests).

32.99%, and 29.48% similarity with foxtail millet (*Setaria italica*) SiNBR1, wheat TaNBR1, rice (*Oryza sativa*) OsNBR1, tobacco (*Nicotiana tabacum*) NtNBR1, and Arabidopsis AtNBR1 proteins, respectively (Figures 2B, S2). We then used RT-qPCR to examine the tissue-specific expression of *ZmNBR1* in different maize tissues. *ZmNBR1* expression was highest in silks, pollen, and leaves and lowest in stems and roots (Figure 2C).

### ZmNBR1 localizes in autophagosomes

NBR1 acts as an autophagy receptor in plants, facilitating degradation of specific substrates, and may be localized in autophagosomes (Su et al., 2021). To determine the subcellular localization of *ZmNBR1*, we transformed the *ZmUbi::ZmNBR1-YFP* and *ZmUbi::AtATG8-mCherry* constructs into maize protoplasts using polyethylene glycol (PEG)-mediated transformation. AtATG8a localizes in autophagosomes and was therefore used as an autophagosome marker (Su et al., 2021). As shown in Figure 2D, we observed a strong yellow fluorescent signal only in maize autophagosomes transformed with the *ZmUbi::ZmNBR1-YFP* construct, whereas we observed fluorescent signals in the cell membrane, cytoplasm, and nucleus of cells transformed with *ZmUbi::YFP* (Figure 2D). These results indicate that *ZmNBR1* localizes in autophagosomes.

### ZmNBR1 enhances drought tolerance in maize

To investigate the role of *ZmNBR1* under drought stress, we generated transgenic plants overexpressing *ZmNBR1* and *ZmNBR1* RNA interference (RNAi) lines, both driven by the maize *Ubiquitin* promoter. *ZmNBR1*-overexpressing lines (OE-*ZmNBR1*#2 and OE-*ZmNBR1*#3) and *ZmNBR1*-knockdown lines (RNAi-*ZmNBR1*#2 and RNAi-*ZmNBR1*#3) were selected and confirmed by RT-qPCR (Figures S3, S4). These transgenic lines together with the empty vector control plants at the three-leaf stage were grown in soil and treated with drought stress for 8 d. We observed no differences in their growth under normal conditions. However, when subjected to drought stress for 8 d, the OE-*ZmNBR1* lines wilted less than the empty vector control plants, whereas the RNAi-*ZmNBR1* lines wilted more and showed stunted growth (Figure 3A). After rewatering and recovery for 3 d, the survival rate of the OE-*ZmNBR1* lines was 80%, while that of the RNAi-*ZmNBR1* lines was 20% compared with the empty vector control plants (Figure 3B). Under the drought condition, the relative water content of the OE-*ZmNBR1* lines was significantly higher than that of the empty vector control plants, but it was significantly lower in the RNAi-*ZmNBR1* lines (Figure 3C). The OE-*ZmNBR1* lines had a slower water loss rate and higher stomatal closure compared with the empty vector control plants, while the RNAi-*ZmNBR1* lines had a greater water loss rate and lower stomatal closure (Figures 3D, S5A). The stomatal density was similar between the three genotypes (Figure S5B), suggesting that *ZmNBR1* enhances drought tolerance by modulating stomatal closure.

To determine the extent of oxidative damage and physiological characteristics of the transgenic plants under drought stress, we measured the percentage of electrolyte leakage, malondialdehyde (MDA) content, and photosynthesis parameters. Under drought stress, the percentage of electrolyte leakage (Figure 3E) and the MDA content (Figure 3F) significantly decreased in the OE-*ZmNBR1* lines but increased in the RNAi-*ZmNBR1* lines compared to the empty vector control plants. Meanwhile, the photosynthetic rate reduced less in the OE-*ZmNBR1* lines and more in the RNAi-*ZmNBR1* lines compared to the empty vector control plants (Figure 3G). In addition, stomatal conductance, the intercellular CO<sub>2</sub> concentration, and the transpiration rate were lower in the OE-*ZmNBR1* lines and higher in the RNAi-*ZmNBR1* lines compared to the empty vector control plants (Figure 3H–J). These results showed that *ZmNBR1* plays a positive role in maize under drought stress.

### ZmNBR1 increases the accumulation of autophagosomes and autophagic activity under drought stress

To investigate the mechanism of *ZmNBR1* in drought stress, we observed autophagosomes in the OE-*ZmNBR1*, RNAi-*ZmNBR1*, and empty vector control plants by MDC staining under drought stress. First, we detected *ZmNBR1* expression in these plants using RT-qPCR at 6 d of drought stress. *ZmNBR1* expression increased 7.4-fold in the OE-*ZmNBR1* lines and 3.7-fold in the empty vector control plants under drought stress, but only 1.5-fold in the RNAi-*ZmNBR1* lines (Figure 4A). This suggested that *ZmNBR1* knockdown reduced *ZmNBR1* expression even under drought stress. We then observed the formation of autophagosomes in leaf cells of these plants. Under normal conditions, autophagosome formation was low in all three genotypes. Under drought stress, the number of autophagosomes was substantially higher in the OE-*ZmNBR1* lines compared with the empty vector control plants. In contrast, the number of autophagosomes was much smaller in the RNAi-*ZmNBR1* lines compared with the empty vector control plants (Figure 4B). We then calculated the relative autophagic activity that the number of autophagosomes divided by the total number of mesophyll cells. Compared with the empty vector control plants, the autophagic activity exhibited a greater increase in the OE-*ZmNBR1* lines and a smaller increase in the RNAi-*ZmNBR1* lines under drought stress (Figure 4C). The ZmATG8a-PE/ZmATG8a ratio increased 5.9-fold in the OE-*ZmNBR1* lines but only 2.1-fold in the RNAi-*ZmNBR1* lines compared to the control condition (Figure 4D, E). Furthermore, the protein level of ZmATG13a increased 2.4-fold in the OE-*ZmNBR1* lines but only 1.3-fold in the RNAi-*ZmNBR1* lines compared to the control condition (Figure 4F, G). These results suggest that *ZmNBR1* improves the accumulation of autophagosomes and autophagic activity under drought stress to enhance drought tolerance in maize.

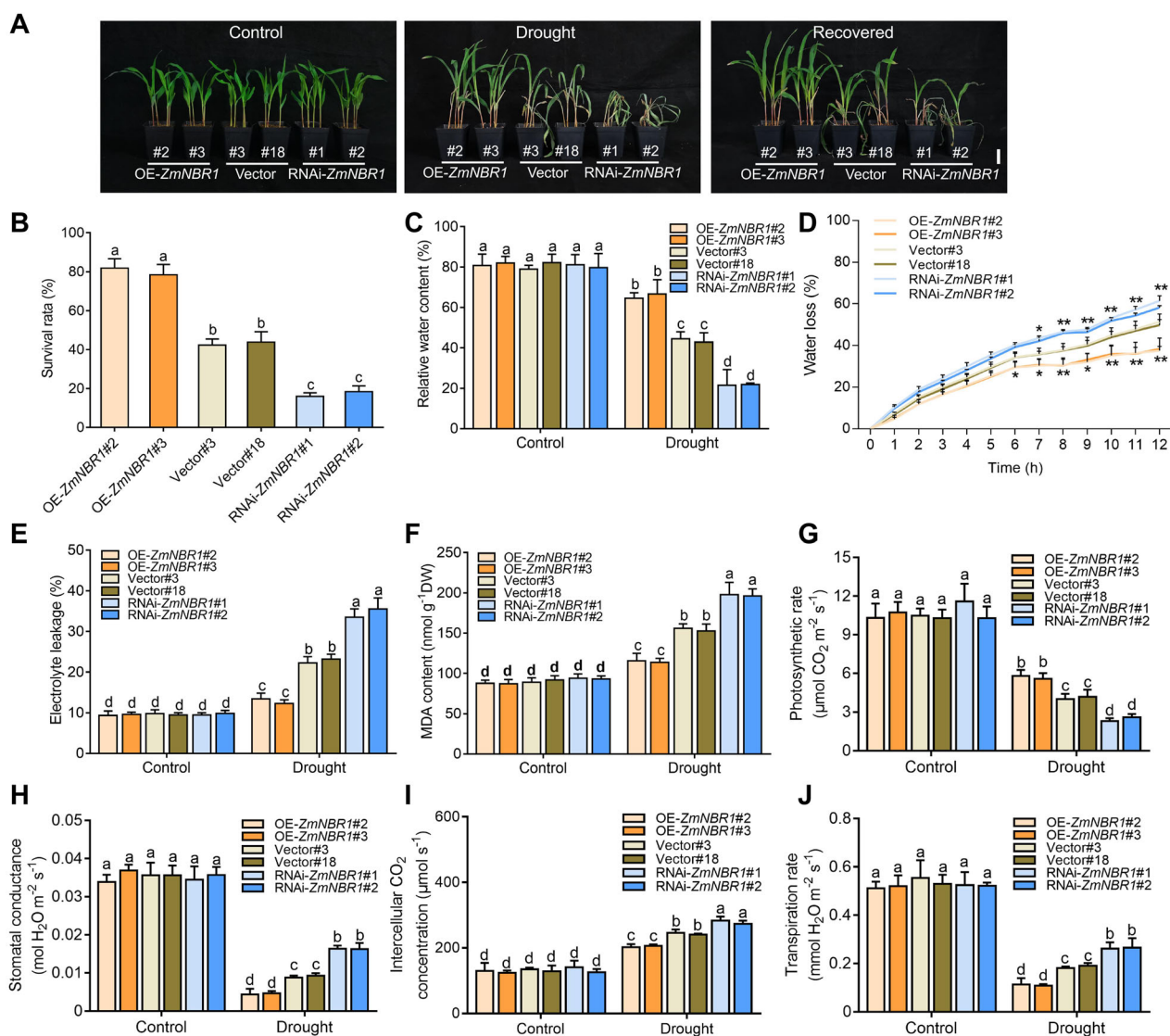


**Figure 3. ZmNBR1 improves the tolerance to drought stress in maize plants**

(A) Phenotypes of the empty vector control plants (Vector#3 and Vector#18), *ZmNBR1*-overexpressing lines (OE-*ZmNBR1*#2 and OE-*ZmNBR1*#3), and *ZmNBR1*-knockdown lines (RNA interference (RNAi)-*ZmNBR1*#1 and RNAi-*ZmNBR1*#2) exposed to drought stress. Plants were grown to the three-leaf stage, treated with or without drought stress for 8 d, and re-watered for 3 d (recovery). Scale bars, 5 cm. (B) Survival rate at the end of the recovery period. (C) Relative water content after 8 d of drought stress. (D) The water loss rate. Second leaves were detached, kept at room temperature, and weighed every hour for 12 h. (E) The percentage of electrolyte leakage, (F) malondialdehyde (MDA) content, (G) photosynthetic rate, (H) stomatal conductance, (I) intercellular CO<sub>2</sub> concentration, and (J) transpiration rate in the leaves of maize plants exposed to drought stress. The three-leaf stage maize plants were treated with or without drought stress for 6 d. Data are means ( $\pm$ SD) of three biological replicates. Different letters indicate significant differences at  $P < 0.05$  according to two-way analysis of variance (Tukey's multiple comparison tests).

### ZmNBR1 affects the expression of genes related to autophagy

Autophagy and autophagosome formation are mediated by a group of genes referred to as autophagy-related genes (ATGs), and the expression of ATG genes is widely used as an indicator for autophagy induction under stress conditions (Sun et al., 2018; Wang et al., 2021; Buerte et al., 2022). We therefore detected the effects of *ZmNBR1* on the expression of genes involved in autophagy. Under drought stress, the OE-*ZmNBR1* lines had 4-fold increased expression of *ZmATG1a* and *ZmATG3*; t3-fold increased expression of *ZmATG6a*, *ZmATG7*,

and *ZmATG13a*; and 6-fold increased expression of *ZmATG8a* and *ZmATG18a* compared with the empty vector control plants. In the RNAi-*ZmNBR1* lines under drought stress, the expression of *ZmATG3*, *ZmATG6a*, *ZmATG7*, and *ZmATG13a* increased 1.6-, 1.4-, 1.3-, and 1.4-fold, respectively, while the expression of both *ZmATG8a* and *ZmATG18a* increased 2-fold compared with the empty vector control plants. *ZmATG1* expression had no changes in the RNAi-*ZmNBR1* lines under drought stress (Figure 5). These results indicate that *ZmNBR1* up-regulates the expression of genes associated with autophagy and enhances autophagic activity under drought stress.



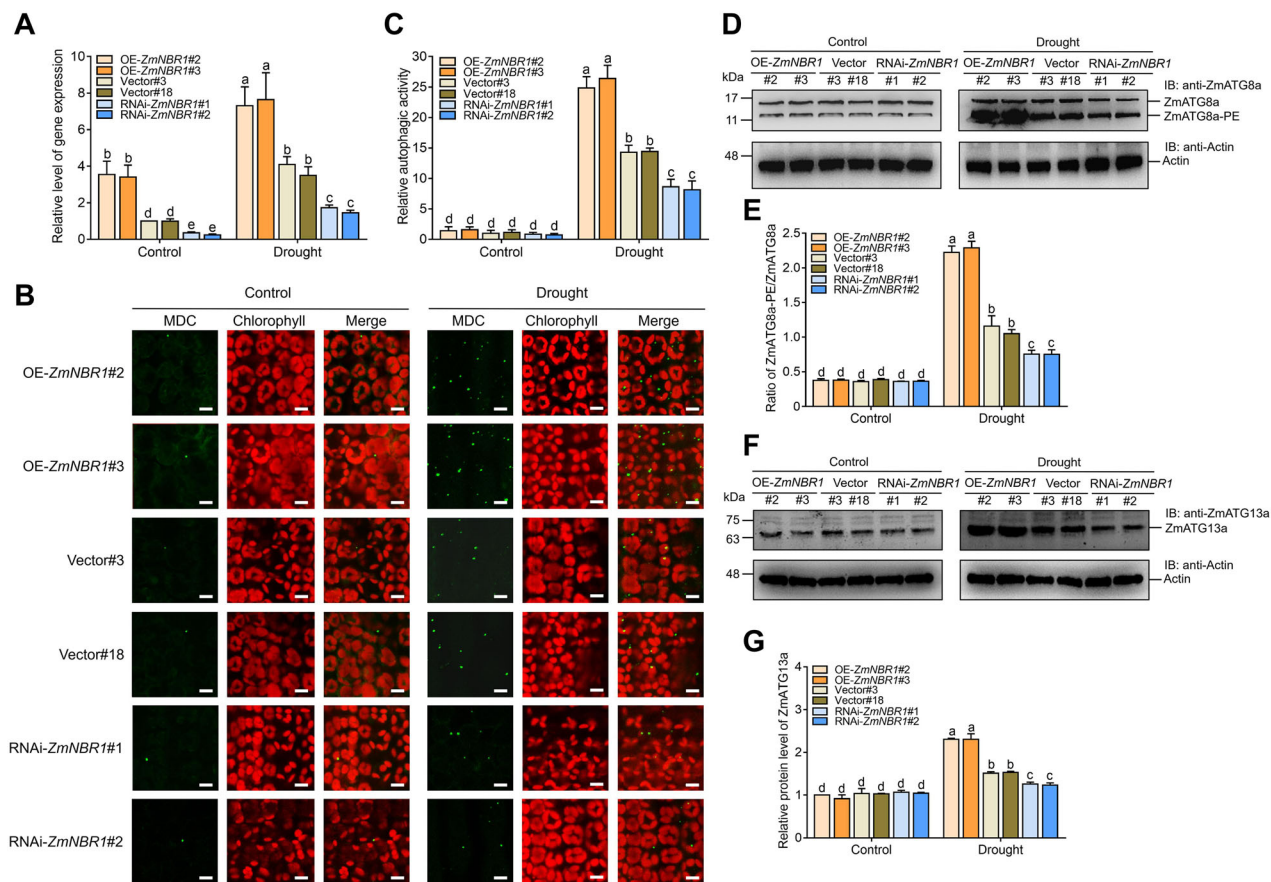


**Figure 4. ZmNBR1 improves the accumulation of autophagosomes and autophagic activity under drought stress**

(A) Expression of *ZmNBR1* in the empty vector control plants (Vector#3 and Vector#18), *ZmNBR1*-overexpressing lines (OE-*ZmNBR1*#2 and OE-*ZmNBR1*#3), and *ZmNBR1*-knockdown lines (RNA interference (RNAi)-*ZmNBR1*#1 and RNAi-*ZmNBR1*#2) exposed to drought stress for 6 d. The values of the empty vector control plants in the control condition were set as 1. *ZmActin* was used as the internal reference. (B) Monodansylcadaverine (MDC) staining in the plants exposed to drought stress for 6 d. Scale bars, 10 μm. (C) The relative autophagic activity of maize plants after 6 d of drought stress treatment as shown in (B). (D) The ratio of ZmATG8a-PE/ZmATG8a in maize leaves under drought stress for 6 d. The proteins were detected with anti-ZmATG8a antibody. ZmActin was used as the loading control. (E) Statistical analysis of the ratio of ZmATG8a-PE/ZmATG8a shown in (D). (F) The protein level of ZmATG13a in maize leaves under drought stress for 6 d. The protein levels were detected with anti-ZmATG13a antibody. ZmActin was used as the loading control. (G) Statistical analysis of ZmATG13a protein level shown in (F). The values of the vector#3 plants in the control condition were set to 1. Data are means ( $\pm$ SD) of three biological replicates. Different letters indicate significant differences at  $P < 0.05$  according to two-way analysis of variance (Tukey's multiple comparison tests).

### ZmNBR1 interacts with ZmBRI1a

To further elucidate the mechanism of *ZmNBR1* in drought tolerance in maize, we performed immunoprecipitation–mass spectrometry (IP-MS) analysis using the OE-*ZmNBR1* lines to identify *ZmNBR1*-interacting proteins. We found that *ZmBRI1a*, a brassinosteroid receptor of the BRI1-like family, interacted with *ZmNBR1*. Co-immunoprecipitation (Co-IP) assays showed that *ZmBRI1a* co-immunoprecipitated with *ZmNBR1* when *Flag-ZmNBR1* was co-expressed with *Myc-ZmBRI1a* but not with *Myc-ZmBSK1* (Figure 6A). Glutathione S-transferase (GST) pull-down assays showed that His-*ZmNBR1* was pulled down by GST-*ZmBRI1a* but not by GST alone (Figure 6B), indicating that *ZmNBR1* interacts with *ZmBRI1a* *in vitro*. In a luciferase complementation imaging (LCI) assay, we observed a strong fluorescence signal when *cLUC-ZmZmNBR1* and *ZmBRI1a-nLUC* were co-infiltrated into *N. benthamiana* leaves (Figure 6C). Furthermore, Proteins, Interfaces, Structures and Assemblies

(PISA) interface analysis showed that the H712 residue in the near-membrane domain of *ZmBRI1a* interacted with the D91 residue in the PB1 domain of *ZmNBR1*. E1055 and D1066 residues in the serine/threonine kinase domain of *ZmBRI1a* were separately bound to H716 and L711 residues of *ZmNBR1*. The K1115, D1117, E1119, and E1120 residues in C-terminal *ZmBRI1a* interacted with R761, R761, E757, and K775 residues in the UBA1 domain of *ZmNBR1*, respectively. The G720 residue of *ZmBRI1a* formed hydrogen bonds with the K817 residue of the UBA2 domain in *ZmNBR1* (Figure S6A; Table S1). LCI assays showed that the near-membrane domain, serine/threonine kinase domain, and C terminus of *ZmBRI1a* were important for the protein interactions between *ZmBRI1a* and *ZmNBR1*. We also found that the UBA1 and UBA2 domains of *ZmNBR1* interacted with *ZmBRI1a* (Figure S6B–E). Together, these results suggest that *ZmNBR1* interacts with *ZmBRI1a* *in vivo* and *in vitro*.

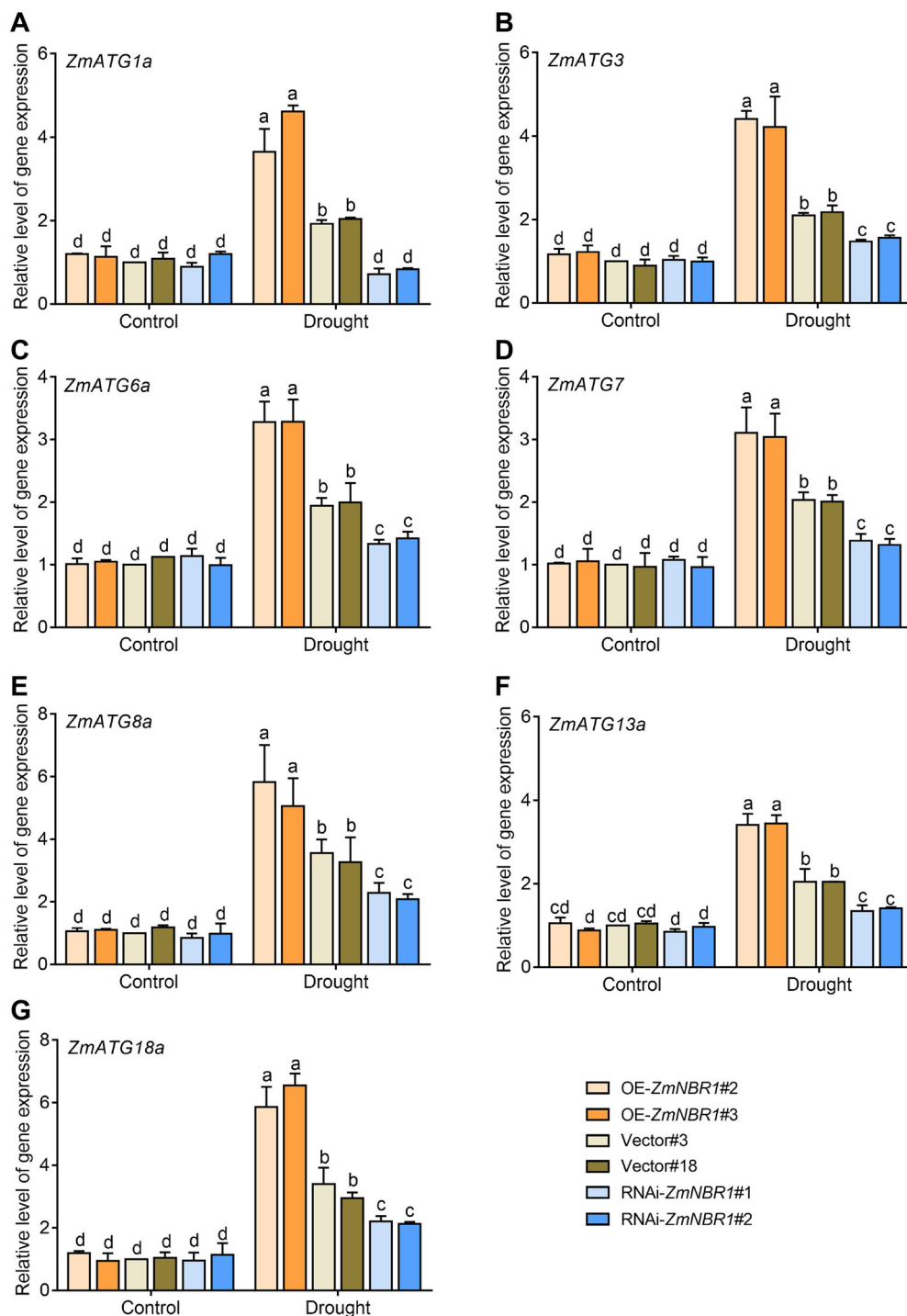


**Figure 5. ZmNBR1 influences the expression of genes related to autophagy in maize**

The expression levels of (A) *ZmATG1a*, (B) *ZmATG3*, (C) *ZmATG6a*, (D) *ZmATG7*, (E) *ZmATG8a*, (F) *ZmATG13a*, and (G) *ZmATG18a* were analyzed in the second leaves of empty vector control plants (Vector#3 and Vector#18), *ZmNBR1*-overexpressing lines (OE-*ZmNBR1*#2 and OE-*ZmNBR1*#3), and *ZmNBR1*-knockdown lines (RNAi-*ZmNBR1*#1 and RNAi-*ZmNBR1*#2) exposed to drought stress for 6 d. The values of the vector#3 plants in the control condition were set as 1. *ZmActin* was used as the internal reference. Data are means ( $\pm$ SD) of three biological replicates. Different letters indicate significant differences at  $P < 0.05$  according to two-way analysis of variance (Tukey's multiple comparison tests).

### ZmBRI1a negatively regulates drought tolerance in maize

To investigate whether *ZmBRI1a* responds to drought stress, we detected *ZmBRI1a* expression during 8 d of

drought treatment. *ZmBRI1a* expression significantly decreased under drought stress compared to levels in the control treatment, beginning at 2 d of treatment and reaching the lowest level at 6 d after the start of drought



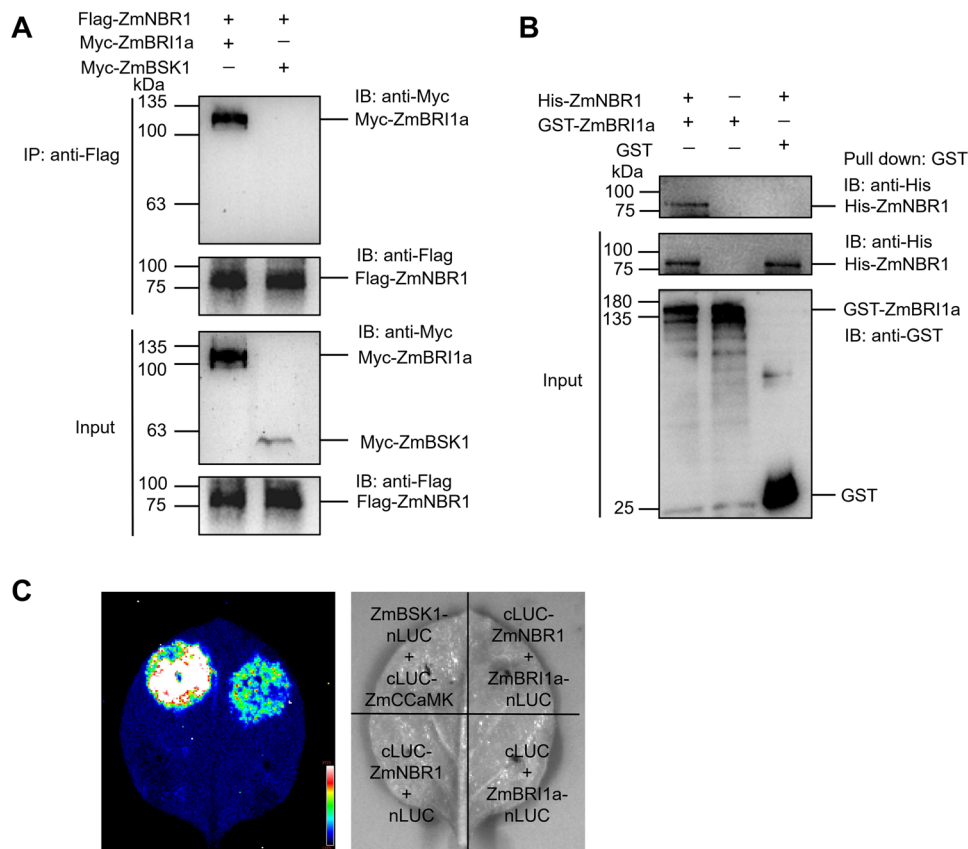


**Figure 6. ZmNBR1 interacts with ZmBRI1a *in vivo* and *in vitro***

**(A)** Co-immunoprecipitation assay confirming the interaction of ZmNBR1 with ZmBRI1a *in vivo*. Flag-ZmNBR1 and Myc-ZmBRI1a were co-expressed in *Nicotiana benthamiana* leaves. Total proteins were extracted from *N. benthamiana* leaves and immunoprecipitated with anti-Flag antibody. Myc-ZmBSK1 was used as the negative control. Flag-ZmNBR1 proteins were detected with anti-Flag antibody. Myc-ZmBRI1a and Myc-ZmBSK1 proteins were detected with anti-Myc antibody. **(B)** Glutathione S-transferase (GST) pull-down assay verifying the interaction of ZmNBR1 with ZmBRI1a *in vitro*. His-ZmNBR1 proteins were incubated with GST-ZmBRI1a or GST proteins in GST magnetic beads. His-ZmNBR1 was detected with anti-His antibody GST and GST-ZmBRI1a were detected with anti-GST antibody. **(C)** Luciferase complementation imaging assay showing the interaction of ZmNBR1 with ZmBRI1a. The cLUC-ZmNBR1 with ZmBRI1a-nLUC constructs were co-transformed in *N. benthamiana* leaves. ZmBSK1-nLUC and cLUC-ZmCCaMK were used as the positive control. Luciferase signals were imaged at 72 h post-transfection.

treatment (Figure S7), indicating that ZmBRI1a expression decreases under drought stress.

To elucidate the function of ZmBRI1a under drought stress, we generated two independent ZmBRI1a-overexpressing lines (OE-ZmBRI1a#2 and OE-ZmBRI1a#4) and ZmBRI1a-knockdown lines (RNAi-ZmBRI1a#3 and RNAi-ZmBRI1a#4) and verified them by RT-qPCR (Figures S8, S9). Under drought stress, the OE-ZmBRI1a lines exhibited greater wilting and the RNAi-ZmBRI1a lines displayed less wilting compared with the empty vector control plants (Figure 7A). The RNAi-ZmBRI1a lines had higher survival rates than the empty vector control plants after re-watering and recovery, while the OE-ZmBRI1a lines had lower survival rates compared to the empty vector control plants (Figure 7B). Moreover, compared to the empty vector control plants, the relative water content and water loss rate were significantly lower in the OE-ZmBRI1a lines and considerably higher in the RNAi-ZmBRI1a lines (Figure 7C, D). The OE-ZmBRI1a lines had lower stomatal closure and higher stomatal density, while the RNAi-ZmBRI1a lines had higher stomatal closure and lower stomatal density compared with the empty vector control plants

(Figure S10). Furthermore, the percentage of electrolyte leakage (Figure 7E) and the MDA content (Figure 7F) were significantly higher in the OE-ZmBRI1a lines but lower in the RNAi-ZmBRI1a lines compared with the empty vector control plants. The photosynthetic rate declined more in the OE-ZmBRI1a lines and less in the RNAi-ZmBRI1a lines than in the empty vector control plants compared with their values in the control condition (Figure 7G). Moreover, stomatal conductance, the intercellular CO<sub>2</sub> concentration, and the transpiration rate were higher in the OE-ZmBRI1a lines and lower in the RNAi-ZmBRI1a lines compared with the empty vector control plants (Figure 7H–J). These results show that ZmBRI1a negatively modulates drought tolerance in maize.

### ZmNBR1 is not phosphorylated by ZmBRI1a, and ZmNBR1 facilitates the autophagic degradation of ZmBRI1a under drought stress

Having confirmed that ZmNBR1 interacts with ZmBRI1a, we tested if ZmNBR1 is phosphorylated by ZmBRI1a using *in vitro* kinase assays. When we incubated GST-ZmBRI1a with the

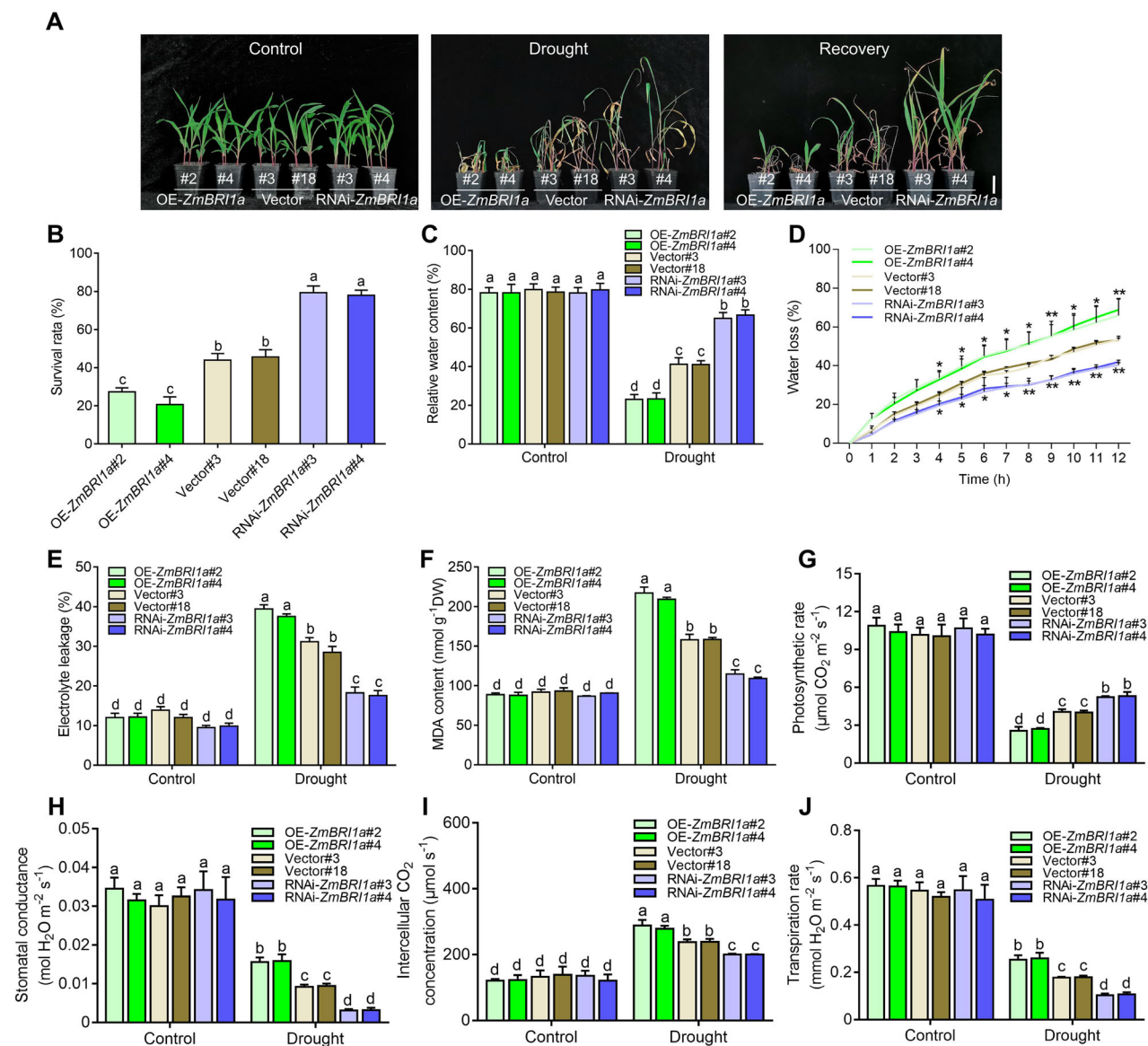


**Figure 7. ZmBRI1a reduces the tolerance to drought stress in maize plant**

(A) Phenotypes of empty vector control plants (Vector#3 and Vector#18), *ZmBRI1a*-overexpressing lines (OE-*ZmBRI1a*#2 and OE-*ZmBRI1a*#4), and *ZmNBR1*-knockdown lines (RNA interference (RNAi)-*ZmNBR1*#3 and RNAi-*ZmNBR1*#4) exposed to drought stress. Plants were grown to the three-leaf stage, treated with or without drought stress for 8 d, and re-watered for 3 d (recovery). Scale bars, 5 cm. (B) Survival rate at the end of the recovery period. (C) Relative water content after 8 d of drought stress. (D) The water loss rate. Second leaves were detached, kept at room temperature, and weighed every hour for 12 h. (E) The percentage of electrolyte leakage, (F) malondialdehyde (MDA) content, (G) photosynthetic rate, (H) stomatal conductance, (I) inter-cellular CO<sub>2</sub> concentration, and (J) transpiration rate in the leaves of maize plants exposed to drought stress. Three-leaf-stage maize plants were treated with or without drought stress for 6 d. Data are means (±SD) of three biological replicates. Different letters indicate significant differences at  $P < 0.05$  according to two-way analysis of variance (Tukey's multiple comparison tests).

general substrate myelin basic protein (MBP), we observed an autophosphorylation band and an MBP phosphorylation band, suggesting that GST-*ZmBRI1a* proteins have kinase activity. However, no phosphorylation band corresponding to His-*ZmNBR1* proteins was observed when we incubated GST-*ZmBRI1a* with His-*NBR1*. The results indicate that *ZmBRI1a* does not phosphorylate *ZmNBR1* (Figure 8A).

To investigate whether *ZmBRI1a* is affected by *ZmNBR1*, we detected the *ZmBRI1a* protein level under drought stress.

Under normal conditions, the *ZmBRI1a* protein level had no change in the OE-*ZmNBR1* plants, the empty vector control plants, and the RNAi-*ZmNBR1* plants. Under drought stress, *ZmBRI1a* protein levels were lower in the OE-*ZmNBR1* plants than in the empty vector control plants and higher in the RNAi-*ZmNBR1* plants (Figure 8B, C).

*NBR1* often functions as an adapter to bridge the interaction between cargo molecules and ATG8 within autophagosomes (Jung et al., 2020; Buerte et al., 2022). To detect

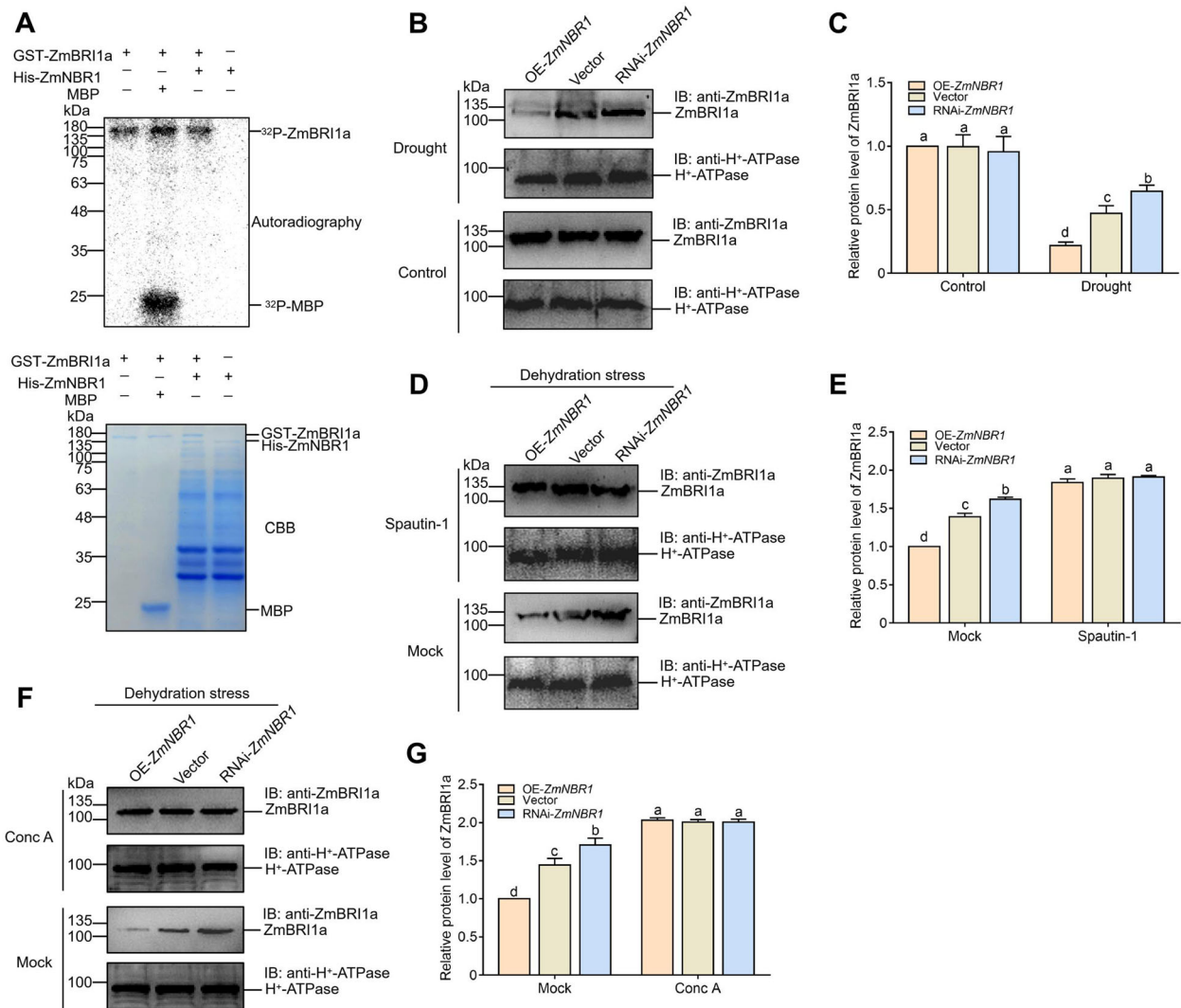


**Figure 8. ZmNBR1 is not phosphorylated by ZmBRI1a, and ZmNBR1 promotes the autophagic degradation of ZmBRI1a**

(A) ZmBRI1a does not phosphorylate ZmNBR1. Glutathione S-transferase (GST)-ZmBRI1a as the kinase and His-ZmNBR1 as the substrate were incubated in kinase reaction buffer at 30°C for 30 min. Myelin basic protein (MBP) was used as a general kinase substrate. The protein inputs were stained by Coomassie brilliant blue (CBB). (B) Immunoblot analysis of the ZmBRI1a protein levels. Plants were grown to the three-leaf stage and then treated with drought stress for 6 d. ZmBRI1a was detected using anti-ZmBRI1a antibody. (C) Statistical analysis of ZmBRI1a protein levels shown in (B). The levels of ZmBRI1a in the OE-ZmNBR1 plants in the control condition were set to 1. (D) Immunoblot analysis of the ZmBRI1a protein levels. Plants were grown to the three-leaf stage and treated with 20% polyethylene glycol (PEG)6000 (dehydration stress) with or without spautin-1 (1 μmol/L) for 12 h. ZmBRI1a was detected using anti-ZmBRI1a antibody. H<sup>+</sup>-ATPase was used as the loading control. (E) Statistical analysis of ZmBRI1a protein levels shown in (D). The protein levels of ZmBRI1a in the OE-ZmNBR1 plants under dehydration stress but lacking spautin-1 were set to 1. (F) Immunoblot analysis of the ZmBRI1a protein levels. Plants were grown to the three-leaf stage and treated with 20% PEG6000 (dehydration stress) with or without concanamycin A (Conc A) (1 μmol/L) for 12 h. ZmBRI1a was detected using anti-ZmBRI1a antibody. H<sup>+</sup>-ATPase was used as the loading control. (G) Statistical analysis of ZmBRI1a protein levels shown in (F). The protein levels of ZmBRI1a in the OE-ZmNBR1 plants under dehydration stress but lacking Conc A were set to 1. Data are means (±SD) of three biological replicates. Different letters indicate significant differences at  $P < 0.05$  according to two-way analysis of variance (Tukey's multiple comparison tests).

whether ZmBRI1a can form a complex with ZmNBR1 and ZmATG8a, we performed GST pull-down and LCI assays. As shown in Figure S11A, His-ZmNBR1 proteins were only pulled down by GST-ZmATG8a but not by GST. In a LCI assay, we observed a strong fluorescence signal when *cLUC-ZmNBR1* and *ZmATG8a-nLUC* were co-infiltrated into *N. benthamiana* leaves (Figure S11C), suggesting that ZmNBR1 interacts with ZmATG8a. Moreover, GST pull-down

and LCI assays showed that ZmATG8a interacted with ZmBRI1a *in vivo* and *in vitro* (Figure S11B, C). These results suggest that ZmBRI1a can form a complex with ZmNBR1 and ZmATG8a. In addition, their interactions were enhanced by PEG6000 treatment (Figure S11D, E). To test whether ZmBRI1a is degraded in the ZmNBR1-mediated autophagic degradation pathway, we used autophagy inhibitor spautin-1, a ubiquitin-specific peptidase (USP10/13) inhibitor that

blocks the autophagic degradation pathway, in OE-*ZmNBR1* and RNAi-*ZmNBR1* plants under dehydration stress. Compared with the empty vector control plants, the ZmBRI1a protein level decreased in the OE-*ZmNBR1* plants, while it increased in the RNAi-*ZmNBR1* plants under dehydration stress. After combining dehydration stress with spautin-1 treatment, the OE-*ZmNBR1* plants had no differences in the ZmBRI1a protein level than that in the empty vector and RNAi-*ZmNBR1* plants (Figure 8D, E).

We then used concanamycin A (Conc A), an inhibitor of vacuolar adenosine triphosphatase (ATPase) that blocks the autophagic degradation pathway, in OE-*ZmNBR1* and RNAi-*ZmNBR1* plants under dehydration stress. The ZmBRI1a protein level was more decreased in OE-*ZmNBR1* plants than in the empty vector control plants, while it was increased in the RNAi-*ZmNBR1* plants under dehydration stress. After combining dehydration stress with Conc A treatment, the OE-*ZmNBR1* plants had no differences in the ZmBRI1a protein level than that in the empty vector control plants and the RNAi-*ZmNBR1* plants (Figure 8F, G). Taken together, these results indicate that ZmNBR1 promotes ZmBRI1a degradation via the selective autophagy pathway under drought stress.

### ZmNBR1 acts genetically upstream of ZmBRI1a in regulating drought tolerance in maize

To characterize the genetic interaction of ZmNBR1 with ZmBRI1a, we crossed the RNAi-*ZmNBR1* and RNAi-*ZmBRI1a* plants to generate RNAi-*ZmNBR1*×RNAi-*ZmBRI1a* plants, which we selected by PCR and confirmed by RT-qPCR (Figure S12). When treated with drought stress, the RNAi-*ZmNBR1*×RNAi-*ZmBRI1a* plants showed enhanced drought tolerance compared to the empty vector control plants and exhibited a drought-tolerant phenotype similar to that of the RNAi-*ZmBRI1a* plants (Figure 9A). The survival rate and relative water content were higher in the RNAi-*ZmNBR1*×RNAi-*ZmBRI1a* plants than in the empty vector control plants and the RNAi-*ZmNBR1* plants under drought stress, while there were no differences between the RNAi-*ZmNBR1*×RNAi-*ZmBRI1a* plants and the RNAi-*ZmBRI1a* plants (Figure 9B, C). Moreover, the RNAi-*ZmNBR1*×RNAi-*ZmBRI1a* plants had a greater water loss rate than the empty vector control plants and the RNAi-*ZmNBR1* plants (Figure 9D). Also, the percentage of electrolyte leakage and MDA content were lower in the RNAi-*ZmNBR1*×RNAi-*ZmBRI1a* and RNAi-*ZmBRI1a* plants than in the empty vector and RNAi-*ZmNBR1* plants (Figure 9E, F). These results showed

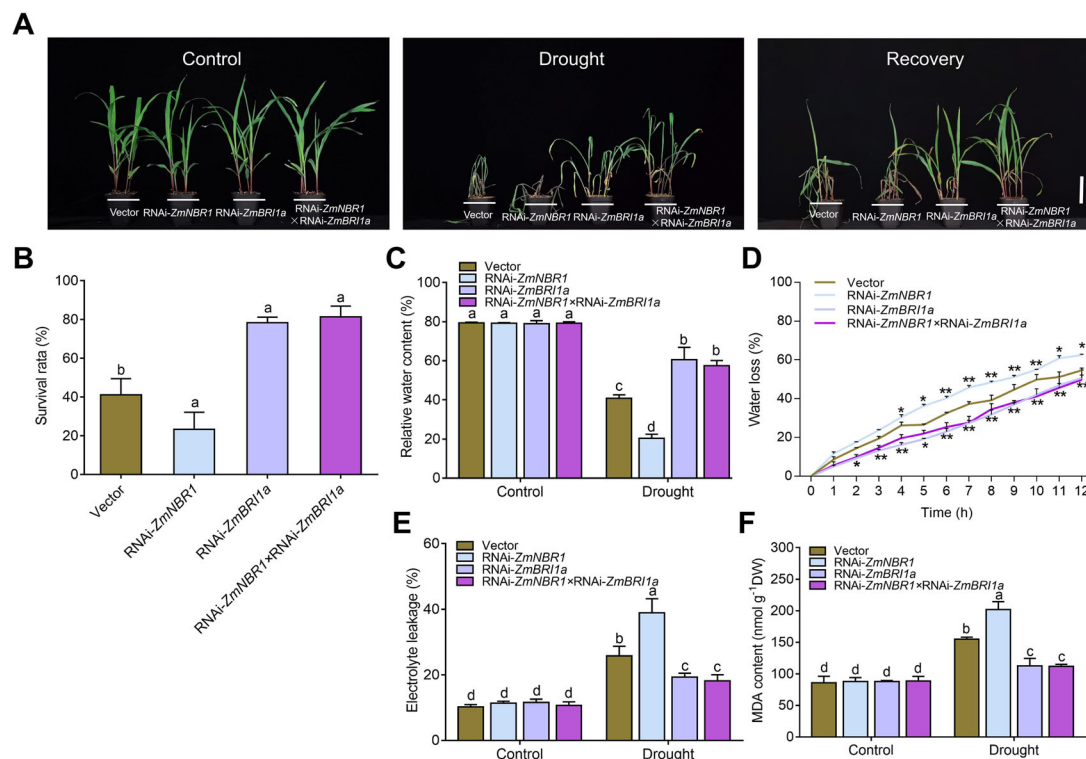


**Figure 9. ZmNBR1 acts genetically upstream of ZmBRI1a in regulating drought tolerance in maize**

Phenotypes of the empty vector control, RNA interference (RNAi)-*ZmNBR1*, RNAi-*ZmBRI1a*, and RNAi-*ZmNBR1*×RNAi-*ZmBRI1a* plants under drought stress. Plants were grown to the three-leaf stage, treated with or without drought stress for 8 d, and re-watered for 3 d (recovery). Scale bars, 5 cm. **(B)** Survival rate at the end of the recovery period. **(C)** Relative water content after 8 d of drought stress. **(D)** The water loss rate. Second leaves were detached and weighed every hour for 12 h. **(E)** The percentage of electrolyte leakage and **(F)** malondialdehyde (MDA) content in the leaves of the maize plants under drought stress. The three-leaf-stage maize plants were treated with or without drought stress for 6 d. Data are means ( $\pm$ SD) of three biological replicates. Different letters indicate significant differences at  $P < 0.05$  according to two-way analysis of variance (Tukey's multiple comparison tests).



that disruption of *ZmBRI1a* in the RNAi-*ZmNBR1* background enhanced drought tolerance and that *ZmBRI1a* acts genetically downstream of *ZmNBR1* in regulating drought tolerance in maize (Figure 10).

## DISCUSSION

Autophagy is induced by drought stress and plays a crucial role in drought tolerance (Wang et al., 2015; Li et al., 2020; Wei et al., 2021; Yu and Hua, 2022). NBR1 functions as a selective autophagy receptor that recognizes and anchors specific ubiquitinated protein substrates and promotes their autophagic degradation (Su et al., 2021; Buerte et al., 2022). In previous studies focused on heat stress, sulfur deficiency, chilling stress, and salt stress, homologs of *NBR1* were found in Arabidopsis (*AtNBR1*), tobacco (*Joka2/NtNBR1*), tomato (*SiNBR1*), poplar (*PagNBR1*), and wheat (*TaNBR1*) in response to abiotic stresses (Zientara-Rytter et al., 2011; Zhou et al., 2013; Chi et al., 2020; Su et al., 2021; Thirumalaikumar et al., 2021). Recently, Chen et al. (2022) identified *TaNBR1* with a similar domain of *NBR1* homologs and found that transgenic Arabidopsis plants overexpressing *TaNBR1* exhibited reduced drought tolerance. However, we showed that the expression of *ZmNBR1*, a maize *NBR1* homolog, was significantly induced by drought stress and that *NBR1* is involved in drought tolerance in maize (Figures 1, 3). Our results, combined with previous studies, suggest that *NBR1* homologs are functionally diverse. In our study, *ZmNBR1* shared only 37.42% similarity with *TaNBR1* (Chen et al., 2022). *ZmNBR1* expression was highest in the silks, while

*TaNBR1* expression was highest in the leaves. In contrast to the subcellular localization of *TaNBR1* in the Golgi apparatus and autophagosomes, *ZmNBR1* localized only to the autophagosomes. Moreover, we found that *ZmNBR1* improves autophagic activity and regulates the expression of genes related to autophagy under drought stress (Figures 4, 5). *ZmNBR1* also affected the expression of the BR pathway-related genes (Figure S13) and the expression of drought-related genes (Figure S15A).

Identification of its substrates is important for *NBR1*-mediated selective autophagy (Ji et al., 2020; Buerte et al., 2022). Although the role of *NBR1* as a selective autophagy receptor was identified, its substrates in plants remained unknown. Recent studies revealed a few specific autophagy substrates of *NBR1* in plant growth, heat stress memory, and abscisic acid (ABA) signaling. For instance, in Arabidopsis, *AtNBR1* anchors exocyst subunit EXO70 family protein E2 (*AtExo70E2*) during autophagy (Ji et al., 2020); and *AtNBR1* interacts with three ABA signaling regulatory proteins, ABSCISIC ACID INSENSITIVE 3 (*ABI3*), *ABI4*, and *ABI5* (Tarnowski et al., 2020). However, the role of *NBR1* in binding specific autophagy substrates in drought stress is not clear.

Here, we identified that *ZmBRI1a*, a BR receptor of the *BRI1*-like family, is a *ZmNBR1*-interacting protein (Figure 6). We found that *ZmBRI1a* expression was down-regulated by drought stress, and *ZmBRI1a* negatively regulates drought tolerance in maize (Figures 7, S7). In addition, *ZmBRI1a* increased oxidative damage and reduced photosynthesis in maize plants under drought stress (Figure 7E–J). *ZmBRI1a* also affected the expression of autophagy- and drought-related genes (Figures S14, S15B). Studies identifying

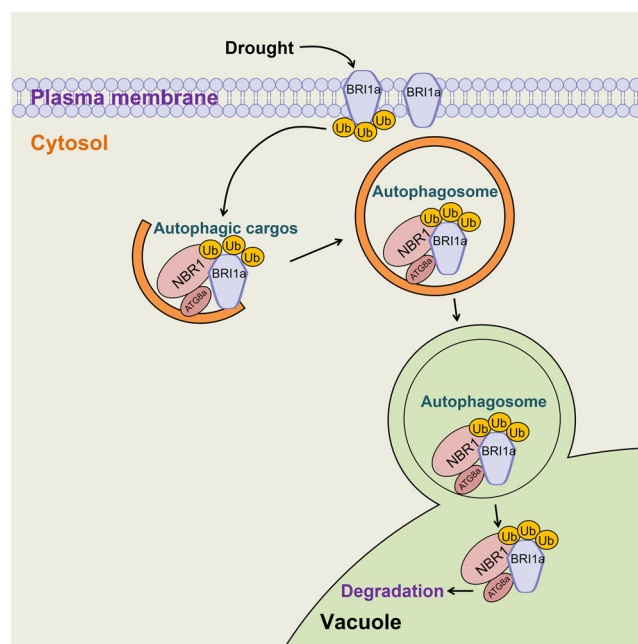


**Figure 10. A working model for *ZmNBR1* mediating the autophagic degradation of *ZmBRI1a* under drought stress**

Under drought stress, *ZmNBR1* regulates the expression of genes related to autophagy to elevate autophagic activity, and promotes the autophagic degradation of *ZmBRI1a* to enhance drought tolerance in maize.

autophagy substrates of NBR1 focused on E2 ubiquitin-conjugating enzymes, chaperones, and transcription factors (Ji et al., 2020; Tarnowski et al., 2020; Thirumalaikumar et al., 2021). A recent study showed that the BR signaling component Brassinazole-resistant 1 (BZR1) participates in NBR1-dependent selective autophagy in response to chilling stress in tomato (Chi et al., 2020), but BZR1 was not a direct autophagy substrate for NBR1. Our findings of the ZmNBR1-interacting protein ZmBRI1a and its role in drought stress extended the understanding that autophagy substrates of NBR1 and other BR signaling components are involved in NBR1-mediated selective autophagy. In addition, ZmBRI1a did not phosphorylate ZmNBR1, and ZmBRI1a acted genetically downstream of ZmNBR1 in regulating maize drought tolerance (Figures 8A, 9).

The BR receptor BRI1 is a single transmembrane, leucine-rich repeat receptor-like kinase (LRR-RLK). The typical structure of BRI1 has an extracellular region and an intracellular region. The extracellular region consists of 25 LRRs, with each LRR containing 25 amino acids. The intracellular region contains a near-membrane domain, a serine/threonine kinase domain that performs BRI1 kinase function, and a C terminus that negatively regulates kinase activity. BRI1 function is initiated by its binding with BR, and activated BRI1 phosphorylates a series of downstream factors to deliver BR signaling (Hothorn et al., 2011; She et al., 2011; Naranjo-Arcos et al., 2023). After BR signaling transduction, excessive BRI1 leads to over-enhanced BR responses. BRI1 internalization and degradation are mainly required for BR signaling attenuation (Zhou et al., 2018; Naranjo-Arcos et al., 2023). Plant U-box 12 (PUB12)/PUB13-mediated ubiquitination of BRI1 is a critical step in its internalization and intracellular degradation (Zhou et al., 2018). In yeast and mammals, ubiquitination modification is recognized by the ubiquitin-binding adaptor proteins Epsin/Eps15-like (Lauwers et al., 2010; Zhou et al., 2018). However, the recognition adaptors of ubiquitinated BRI1 in plants have not yet been characterized.

In this study, we demonstrated that ZmNBR1 interacts with ZmBRI1a and ZmATG8a and that ZmBRI1a is degraded by the NBR1-mediated selective autophagy pathway under drought stress (Figures 6, 8B–G, S11). PISA interface analysis and LCI assays showed that the near-membrane domain, serine/threonine kinase domain, and C terminus of ZmBRI1a are important for the protein interactions between ZmBRI1a and ZmNBR1 (Figure S6A–E; Table S1). NBR1 functions as a selective autophagy receptor and anchors ubiquitinated proteins via its C-terminal UBA1 and UBA2 domains for degradation (Lamark et al., 2009; Jung et al., 2020; Zhang and Chen, 2020; Su et al., 2021; Buerte et al., 2022; Akhter et al., 2023). In this study, we found that the UBA1 and UBA2 domains of ZmNBR1 interact with ZmBRI1a (Figure S6B–E). Therefore, ZmNBR1 binds the near-membrane domain, serine/threonine kinase domain, and C terminus of ubiquitinated ZmBRI1a via its PB1 domain and C-terminal UBA domains. ZmNBR1 then promotes ubiquitinated ZmBRI1a to

enter the NBR1-mediated selective autophagic pathway for degrading ZmBRI1a under drought stress.

In addition, our results show that ZmNBR1 positively regulates, while ZmBRI1a negatively regulates drought tolerance in maize (Figures 3, 7). Fabregas et al. (2018) showed that the *bri1* mutant had enhanced drought tolerance in Arabidopsis. Enhancing BR signaling with *SIBRI1* overexpression negatively modulated tomato drought tolerance, and the BR content increased in *SIBRI1*-overexpressing tomato plants under drought stress (Nie et al., 2019). This indicates that drought stress regulates BR signaling intensity via BRI1. Excessive BRI1 resulted in over-enhanced BR responses and decreased drought tolerance. In our study, ZmNBR1 interacted with ZmBRI1a to degrade ZmBRI1a under drought stress, which may attenuate BR signaling. This may explain how the over-reactive BR response is slowed down, thus enhancing plant drought tolerance. A recent study also showed that the *bri1*-associated receptor kinase (*bak1*) and *bri1-301* mutants are more sensitive to drought stress (Deng et al., 2022), suggesting the complexity of BR signaling in regulating plant drought tolerance. The relationship between BR receptors and drought stress needs to be further explored.

In summary, our results showed that ZmNBR1 regulates the expression of genes related to autophagy to elevate autophagic activity, and promotes the autophagic degradation of ZmBRI1a to enhance maize drought tolerance.

## MATERIALS AND METHODS

### Plant materials and treatments

Maize (*Z. mays* L. cv. B73) plants were grown at 28°C d/22°C night. The photoperiod was 14 h d/10 h night, and photosynthetically active radiation was 200  $\mu\text{mol m}^{-2} \text{s}^{-1}$ . The three-leaf-stage maize plants were subjected to drought stress or distilled water (control) for various durations (0, 2, 4, 6, and 8 d). The relative soil moisture levels during the drought stress treatment are shown in Figure S16. Second leaves were collected for analysis.

To detect the tissue-specific expression pattern of *ZmNBR1*, root, stem, and leaf samples were collected from the three-leaf-stage maize plants, while silk and pollen were collected at the flowering stage.

For generating *ZmNBR1*- and *ZmBRI1a*-overexpressing maize plants, full-length *ZmNBR1* and *ZmBRI1a* were cloned and amplified by specific primers (Table S2). The sequences of *ZmNBR1* and *ZmBRI1a* were constructed into the pCUN-NHF vector driven by the maize *Ubiquitin* promoter using the ClonExpressII One Step Cloning Kit according to the manufacturer's protocol (Vazyme, China). For generating *ZmNBR1*-knockdown maize plants, a sequence containing two specific reverse-complementary fragments (400 bp) linked with a 400-bp  $\beta$ -glucuronidase (GUS) intron sequence (Figure S3) was inserted into the pCUN-NHF vector. For generating *ZmBRI1a*-knockdown maize plants, a sequence containing two specific

fragments (200 bp) linked with a 400-bp GUS intron sequence (Figure S8) was inserted into the pCUN-NHF vector. The transgenic maize plants were generated as described in detail by Xiang et al. (2021a). Two independent homozygous T<sub>2</sub> lines of each genotype were chosen for subsequent analyses.

### Monodansylcadaverine staining

The second leaves of three-leaf-stage maize plants were placed in phosphate-buffered saline (PBS) containing 50 µmol/L MDC and then vacuumed at 0.1 MPa for 30 min at room temperature and kept away from light. Leaves were washed in PBS and observed using a confocal laser scanning microscope (Zeiss LSM 780; Carl Zeiss, Gottingen, Germany). The excitation wavelength was set at 405 nm, and the emission wavelength was set at 420–485 nm. The relative autophagic activity was counted and calculated using ImageJ software. The number of autophagosomes divided by the total number of mesophyll cells represented the relative autophagic activity.

### Alignment and phylogenetic analysis of ZmNBR1

Sequences of NBR1 proteins were obtained from the National Center for Biotechnology Information (NCBI) database (<https://www.ncbi.nlm.nih.gov/>) and aligned by DNAMAN software (version 5.0; LynnonBiosoft, USA). The protein sequence similarity was counted by DNAMAN software (version 6). A phylogenetic tree of NBR1 proteins was drawn using MEGA software (version 5.0; Mega, Raynham, MA, USA). The phylogenetic relationship was conducted using the neighbor-joining method with *p*-distance correction. Bootstrap values were calculated from 1,000 replicate runs.

### Reverse transcription-qPCR analysis

Total RNA was extracted using TRIzol Reagent (CoWin Biotech, Shanghai, China) and reverse-transcribed into complementary DNA (cDNA) using the 5×All-In-One MasterMix Kit according to the manufacturer's protocol (Applied Biological Materials Inc., Zhenjiang, China). The relative expression of genes was detected by CFX96 Touch Real-Time PCR System (Bio-Rad, Hercules, CA, USA) using Hieff qPCR SYBR Green Master Mix (Yeasen, Shanghai, China) with specific primers (Table S2). *ZmActin* was used as the internal reference. Relative gene expression was assessed by the  $2^{-\Delta\Delta CT}$  method.

### Immunoblot analysis

Proteins were extracted with extracting buffer (10 mmol/L Tris-HCl pH 7.5, 150 mmol/L NaCl, 5 mmol/L ethylenediaminetetraacetic acid (EDTA), 1% Triton X-100, 0.1% sodium dodecyl sulfate (SDS), 0.5 mmol/L dithiothreitol (DTT), and 1× Yeasen InStab Protease Inhibitor Cocktail). The protein samples were centrifuged at 12,000 *g* for 20 min, and supernatants were collected. Protein samples (100 µg) were boiled for 10 min with addition of 5 µL 5× SDS loading buffer. Protein samples were separated by 12% SDS polyacrylamide gel electrophoresis (SDS-PAGE). To detect ZmATG8a-PE (lipidation form), the protein samples were separated by 15% SDS-PAGE with 6 mol/L urea according to the method of Qi et al. (2023). Proteins were

transferred onto polyvinylidene fluoride (PVDF) membranes. The PVDF membranes were blocked with 5% skimmed milk at room temperature for 2 h and incubated with primary antibodies overnight at 4°C. Then, the membranes were incubated with horseradish peroxidase (HRP)-conjugated secondary antibodies (1:5,000; Abmart, Shanghai, China) for 2 h at room temperature. Protein immunoblot signal was detected with the enhanced chemiluminescence substrate (Super ECL Detection Reagent; Yeasen, Shanghai, China) using a 5200 multi-chemiluminescent imaging system (Tanon, Shanghai, China). Anti-ZmATG8a (Cat. No. ab77003, 1:1,000; Abcam, UK), anti-ZmATG13a (Cat. No. AS194279, 1:1,000; Agrisera, Sweden), anti-Flag (mouse mAb; Cat. No. M20008, 1:2,000; Abmart, Shanghai, China), anti-Flag (rabbit mAb; Cat. No. 30504ES50, 1:2,000; Yeasen, Shanghai, China), anti-Myc (Cat. No. T62076, 1:2,000; Abmart, Shanghai, China), anti-ZmBRI1a (Cat. No. A20670, 1:2,000; ABClonal, Wuhan, China), anti-His (Cat. No. M20001, 1:1,000; Abmart, Shanghai, China), anti-GST (Cat. No. M20007, 1:1,000; Abmart, Shanghai, China), anti-H<sup>+</sup>-ATPase (Cat. No. PHY0032, 1:1,000; PhytoAB, San Jose, CA, USA), and anti-ZmActin (Cat. No. B1051, 1:2,000; Biodragon, Suzhou, China) antibodies were used. Quantification of the protein immunoblot signal was measured with ImageJ version 1.54f software (<https://imagej.net/software/imagej/>).

### RNA sequencing analysis

The three-leaf-stage maize seedlings were treated with drought stress for 4 d. The second leaves were sampled for RNA extraction. RNA integrity was evaluated using an Agilent Bioanalyzer 2100 system (Agilent Technologies, Santa Clara, CA, USA). Library construction and transcriptome sequencing were performed by Novogene (Beijing, China). Data analysis was performed using Novomagic, an online platform for data analysis (Novogene; <https://magic.novogene.com>). Briefly, Pearson's correlation analysis was performed to analyze the correlation between all biological replicate samples. Differential expression analysis was performed using the DESeq. 2R package (1.20.0). DEGs were identified with the set criteria of  $|\log_2 \text{Fold Change}| > 1$  and  $P < 0.05$ . KEGG enrichment analysis was performed using the clusterProfiler R package. A heatmap of the expression levels of the DEGs was performed using R (version 3.0.3) ggplot2 and heatmap package.

### Subcellular localization

The sequence of *ZmNBR1* was inserted into the pXZP008-YFP vector. The *ZmUbi:ZmNBR1-YFP* and empty vector *ZmUbi:YFP* together with *ZmUbi:AtATG8a-mCherry* constructs were transfected into maize protoplasts. *ZmUbi:AtATG8a-mCherry* was used as an autophagosome localization marker (Luan et al., 2021; Su et al., 2021). The extraction and PEG-mediated transformation method of maize protoplasts were performed as previously described (Xiang et al., 2021b). The yellow fluorescence signal was observed and imaged using a confocal laser scanning microscope (Zeiss LSM 780; Carl Zeiss, Gottingen, Germany) after a 16-h incubation.

### Phenotype analysis

The three-leaf-stage maize seedlings of the empty vector control plants, the *ZmNBR1*-overexpressing lines, and the *ZmNBR1*-knockdown lines were treated with drought stress by withholding water for 8 d. After drought treatment, the maize plants were re-watered and recovered for 3 d. The drought-tolerant phenotypes of the seedlings were observed and photographed. The survival rate was measured. The relative water contents of maize plants after 8 d of drought treatment were measured as described by Yoo et al. (2010).

### Physiological measurements

The water loss rate of detached leaves was assessed as previously described with some modifications (Deng et al., 2022). The second leaves were cut from three-leaf-stage maize plants and weighed every hour for 12 h at room temperature. Analysis of stomatal density was performed as described by Xiang et al. (2021a). Analysis of stomatal closure was performed as described by Wang et al. (2023). The second leaves were cut from three-leaf-stage maize plants, boiled for 10 min to fix cells, and decolorized in 75% ethanol overnight. The decolorized leaves were placed in a clearing solution (glycerol:chloral hydrate: water, 1:8:1 (v/w/v)) overnight. The status of stomatal closure and stomatal types were observed using a fluorescence microscope (Axio Image A1; Carl Zeiss, Gottingen, Germany).

The three-leaf-stage maize plants were treated with drought stress for 6 d. The second leaves were sampled to determine the percentage of electrolyte leakage and the MDA content as previously described (Xiang et al., 2021b).

To measure photosynthesis parameters, the three-leaf-stage maize plants were treated with drought stress for 6 d. The photosynthetic rate, stomatal conductance, intercellular CO<sub>2</sub> concentration, and transpiration rate were determined using a Li-Cor 6400 Portable Photosynthesis System (Li-Cor Inc., Lincoln, NE, USA) as described by Yoo et al. (2010) and Xiang et al. (2021a).

### Immunoprecipitation-MS

Total proteins were extracted from the OE-*ZmNBR1* lines using extraction buffer (10 mmol/L Tris-HCl pH 7.5, 150 mmol/L NaCl, 5 mmol/L EDTA, 1% Triton X-100, 0.1% SDS, 0.5 mmol/L DTT, and 1× Yeasen InStab Protease Inhibitor Cocktail). Protein extracts (200 µg) were immunoprecipitated with anti-Flag antibody (1:1,000; Yeasen, Shanghai, China) in IP buffer (20 mmol/L Tris-HCl, pH 7.5, 20 mmol/L KCl, 150 mmol/L NaCl, 10 mmol/L MgCl<sub>2</sub>, and 1× Yeasen InStab Protease Inhibitor Cocktail). The protein-flag complexes were bound to Protein A/G MagBeads. The beads were washed three times with IP buffer. The protein samples were digested using Trypsin/Lys-C Mix (20 ng/µL) (Promega, Madison, WA, USA). The cleaved peptides were analyzed using the Nano LC-LTQ Orbitrap XL Liquid Chromatography – tandem mass spectrometry (LC-MS/MS) System (Thermo Scientific, Waltham, MA, USA). Data were analyzed using pFindStudio software (v.3.1.6) (Chi et al., 2018).

### Co-immunoprecipitation assays

Full-length *ZmNBR1* sequences were inserted into the pCambia1300-221-3×Flag vector. Full-length *ZmBRI1a* sequences were inserted into the pCambia1300-221-6×Myc vector. The vector constructions were performed with the ClonExpressII One Step Cloning Kit according to the manufacturer's instructions (Vazyme, Nanjing, China). The recombinant vectors were transformed into *N. benthamiana* leaves using *Agrobacterium tumefaciens* strain GV3101 infiltration. After incubation for 3 d, total proteins were extracted from *N. benthamiana* leaves with extraction buffer (10 mmol/L Tris-HCl pH 7.5, 150 mmol/L NaCl, 5 mmol/L EDTA, 1% Triton X-100, 0.1% SDS, 0.5 mmol/L DTT, and 1× Yeasen InStab Protease Inhibitor Cocktail). Protein samples were immunoprecipitated with anti-Flag antibody (1:1,000; Yeasen, Shanghai, China) in IP buffer (20 mmol/L Tris-HCl, pH 7.5, 20 mmol/L KCl, 150 mmol/L NaCl, 10 mmol/L MgCl<sub>2</sub>, and 1× Yeasen InStab Protease Inhibitor Cocktail). The protein-flag complexes were bound to Protein A/G MagBeads for 2 h. The complexes were washed three times and boiled with 5× SDS loading buffer for 5 min. Protein samples were separated by 12% SDS-PAGE. Myc-ZmBRI1a was detected with anti-Myc antibody. Flag-ZmNBR1 was detected with anti-Flag antibody.

### Glutathione S-transferase pull-down assays

Full-length *ZmNBR1* and *ZmATG8a* sequences were inserted into the pET-30a vector. Full-length *ZmBRI1a* and *ZmATG8a* sequences were inserted into the pGEX-4T-1 vector. The recombinant vectors were transformed into *Escherichia coli* Rosetta (DE3) cells. Recombinant proteins were expressed for 6 h at 28°C induced by 0.5 mmol/L isopropyl-1-thio-β-D-galactopyranoside (IPTG). The proteins were purified using the MagnetGST or MagnetHis protein purification system (Promega, Madison, WA, USA). His-ZmNBR1 and His-ZmATG8a proteins were incubated with GST-ZmBRI1a, GST-ZmATG8a, or GST proteins in GST magnetic beads. Protein samples were separated by 12% SDS-PAGE. His-ZmNBR1 or His-ZmATG8a proteins were detected with anti-His antibody (1:1,000; Abmart, Shanghai, China). GST, GST-ZmBRI1a, and GST-ZmATG8a proteins were detected with anti-GST antibody (1:1,000; Abmart, Shanghai, China).

### Luciferase complementation imaging assays

Full-length *ZmNBR1* and its derivative sequences and *ZmATG8a* sequences were inserted into the pCambia1300-cLUC vector. Full-length *ZmBRI1a* and its derivative sequences and *ZmATG8a* sequences were inserted into the pCambia1300-nLUC vector. The constructs were transformed into *A. tumefaciens* strain GV3101. The bacteria were injected into *N. benthamiana* leaves. At 72 h post-transfection, the LUC signal was observed and imaged using a Tanon 5200 multi-chemiluminescent imaging system (Tanon, Shanghai, China). *ZmBSK1-nLUC* and *cLUC-ZmCCaMK* were used as the positive control (Liu et al., 2021).



### In vitro kinase assays

The His-ZmNBR1 and GST-ZmBRI1a proteins were expressed and purified as described in the section on GST pull-down assays. The GST-ZmBRI1a proteins (1 µg) were incubated with general substrate MBP (1 µg) or His-ZmNBR1 proteins (2 µg) in kinase reaction buffer (20 mmol/L Tris-HCl pH 7.5, 100 mmol/L NaCl, 12 mmol/L MgCl<sub>2</sub>, 1 µCi [ $\gamma$ -<sup>32</sup>P]-ATP) at 30°C for 30 min. After incubation, the reaction was terminated by adding 4 µL 5× SDS loading buffer. Protein samples were boiled for 5 min and separated by 12% SDS-PAGE. PAGE gels were washed twice for 10 min each with trichloroacetic acid (TCA) solution (5% TCA, 1% NaPPi). Then, gels were wrapped in dialysis glassine paper and naturally dried. Dried gels were scanned by Typhoon Trio multifunctional laser scanning imager (General Electric, Fairfield, CT, USA). The protein inputs were stained by Coomassie brilliant blue (CBB).

### Dehydration stress and autophagy inhibitor treatment

The three-leaf-stage maize plants were treated with 20% PEG6000 for dehydration stress. For autophagy inhibitor treatment, dimethyl sulfoxide, spautin-1 (1 µmol/L; Yuanye Biotechnology, Shanghai, China), or Conc A (1 µmol/L; GLP BIO, Montclair, CA, USA) was added to the PEG6000 treatment for 12 h. Total proteins were extracted and separated as described in the section on Co-IP assays. ZmBRI1a was detected using anti-ZmBRI1a antibody. H<sup>+</sup>-ATPase was used as the loading control.

### Proteins, Interfaces, Structures and Assemblies interface analysis

The protein structure was built using the Colab website AlphaFold2 online (<https://colab.research.google.com/github/sokrypton/ColabFold>). The structure of protein-coding sequences was constructed as described by Mirdita et al. (2022). The analysis of crystal interfaces was conducted using PISA interface analysis ([https://www.ebi.ac.uk/msd-srv/prot\\_int/picite.html](https://www.ebi.ac.uk/msd-srv/prot_int/picite.html)). The method of PISA interface analysis was previously described (Krissinel and Henrick, 2007).

### Statistical analysis

All data were analyzed using GraphPad Prism version 7.0 software (GraphPad Software, San Diego, CA, USA). Statistical significance was determined by one- or two-way analysis of variance corrected with Tukey's multiple comparison tests. Differences were considered significant at  $P < 0.05$ .

### Accession numbers

The gene sequences in this study have the following IDs: *ZmNBR1*, GRMZM2G092447; *SbNBR1*, XP\_002454107; *SiNBR1*, XP\_004952961; *OsNBR1*, XP\_015625351; *TaNBR1*, QEE80346; *AtNBR1*, NP\_194200; *NtNBR1*, XP\_016458014; *ZmATG1*, GRMZM2G105415; *ZmATG3*, GRMZM5G818887; *ZmATG6a*, GRMZM2G092112; *ZmATG7*, GRMZM2G005304; *ZmATG8a*, GRMZM2G336871; *ZmATG13a*, GRMZM2G00973; *ZmATG18a*, GRMZM2G122607; *ZmActin*, EU952376;

*ZmBRI1a*, Zm00001d011721; *ZmDWF4*, GRMZM2G065635; *ZmDET2*, GRMZM2G449033; *ZmCPD*, GRMZM2G107199; *ZmBSK1*, GRMZM2G127050; *ZmBSU1*, GRMZM2G148539; *ZmBIN2*, GRMZM2G472625; *ZmBZR1*, GRMZM5G812774; *ZmDREB2.9*, Zm00001d008665; *ZmPIP1.2*, Zm00001d017526; *ZmPIP2.5*, GRMZM2G178693; *ZmRD20*, GRMZM2G166281.

### Data availability statement

RNA-seq data of the three-leaf-stage maize seedlings treated with drought stress in this study are available from the NCBI under the BioProject PRJNA1092742.

## ACKNOWLEDGEMENTS

This study was supported by National Natural Science Foundation of China (32201707), Natural Science Foundation of Jiangsu Province (BK20220999), the Fundamental Research Funds for the Central Universities (KYQN2023025), China Postdoctoral Science Foundation (2021M701739, 2023T160323), Jiangsu Funding Program for Excellent Postdoctoral Talent (2022ZB330), Open Competition Mechanism to Select the Best Candidates Fund of Jiangsu Province (JBGS[2021]012), Key Research and Development Program of Ningxia Hui Autonomous Region (2023BCF01009), and the Achievement Transformation Fund Project of Hainan Research Institute of Nanjing Agricultural University (NAUSY-CG-YB07).

## CONFLICT OF INTEREST

The authors declare no conflict of interest.

## AUTHOR CONTRIBUTIONS

A.Z. and Y.X. conceived the project, designed the experiments, and wrote the manuscript; Y.X., G.L., Q.L., and Y.N. performed most of the experiments; Y.P., Y.C., and X.B. helped with the phenotype analysis and data curation; C.Z. and Y.W. helped with vector constructions. All authors read and approved the contents of this paper.

**Edited by:** Zhizhong Gong, China Agricultural University, China

**Received** Dec. 16, 2023; **Accepted** Mar. 26, 2024; **Published** Apr. 12, 2024

## REFERENCES

- Akhter, D., Zhang, Y., Hu, J., and Pan, R. (2023). Protein ubiquitination in plant peroxisomes. *J. Integr. Plant Biol.* **65**: 371–380.
- Bao, Y., Song, W.M., Wang, P., Yu, X., Li, B., Jiang, C., Shiu, S.H., Zhang, H., and Bassham, D.C. (2020). COST1 regulates autophagy to

- control plant drought tolerance. *Proc. Nat. Acad. Sci. U.S.A.* **117**: 7482–7493.
- Buerte, B., Zeng, Z., Zhou, C., Lian, G., Guo, F., Wang, J., Han, N., Zhu, M., and Bian, H. (2022). Identification of new ATG8s-binding proteins with canonical LC3-interacting region in autophagosomes of Barley Callus. *Plant Cell Physiol.* **63**: 508–520.
- Chen, L., Lv, Q., Yang, W., Yang, H., Chen, Q., Wang, B., Lei, Y., and Xie, Y. (2022). TaNBR1, a novel wheat NBR1-like domain gene negatively regulates drought stress tolerance in transgenic Arabidopsis. *Int. J. Mol. Sci.* **23**: 4519.
- Chi, C., Li, X., Fang, P., Xia, X., Shi, K., Zhou, Y., Zhou, J., and Yu, J. (2020). Brassinosteroids act as a positive regulator of NBR1-dependent selective autophagy in response to chilling stress in tomato. *J. Exp. Bot.* **71**: 1092–1106.
- Chi, H., Liu, C., Yang, H., Zeng, W.F., Wu, L., Zhou, W.J., Wang, R.M., Niu, X.N., Ding, D.Y., Zhang, Y., et al. (2018). Comprehensive identification of peptides in tandem mass spectra using an efficient open search engine. *Nat. Biotechnol.* **36**: 1059–1061.
- Dagdas, Y.F., Khaoula, B., Abbas, M., Angela, C.G., Pooja, P., Benjamin, P., Nadra, T., Neftaly, C.M., Hughes, R.K., and Jan, S. (2016). An effector of the Irish potato famine pathogen antagonizes a host autophagy cargo receptor. *eLife* **5**: e10856.
- Deng, J., Kong, L., Zhu, Y., Pei, D., Chen, X., Wang, Y., Qi, J., Song, C., Yang, S., and Gong, Z. (2022). BAK1 plays contrasting roles in regulating abscisic acid-induced stomatal closure and abscisic acid-inhibited primary root growth in Arabidopsis. *J. Integr. Plant Biol.* **64**: 1264–1280.
- Fabregas N., Lozano-Elena F., Blasco-Escamez D., Tohge T., Martinez-Andujar C., Albacete A., Osorio S., Bustamante M., Riechmann J.L., Nomura T., et al. (2018). Overexpression of the vascular brassinosteroid receptor BRL3 confers drought resistance without penalizing plant growth. *Nat. Commun.* **9**: 4680.
- Hafrén, A., Macia, J.L., Love, A.J., Milner, J.J., Drucker, M., and Hofius, D. (2017). Selective autophagy limits cauliflower mosaic virus infection by NBR1-mediated targeting of viral capsid protein and particles. *Proc. Nat. Acad. Sci. U.S.A.* **114**: e2026–e2035.
- Hothorn, M., Belkadir, Y., Dreux, M., Dabi, T., Noel, J.P., Wilson, I.A., and Chory, J. (2011). Structural basis of steroid hormone perception by the receptor kinase BRI1. *Nature* **474**: 467–471.
- Ji, C., Zhou, J., Guo, R., Lin, Y., Kung, C.H., Hu, S., Ng, W.Y., Zhuang, X., and Jiang, L. (2020). AtNBR1 is a selective autophagic receptor for AtExo70E2 in Arabidopsis. *Plant Physiol.* **184**: 777–791.
- Jia, X., Gong, X., Jia, X., Li, X., Wang, Y., Wang, P., Huo, L., Sun, X., Che, R., Li, T., et al. (2021). Overexpression of MdATG8i enhances drought tolerance by alleviating oxidative damage and promoting water uptake in transgenic apple. *Int. J. Mol. Sci.* **22**: 5517.
- Jung, H., Lee, H.N., Marshall, R.S., Lomax, A.W., Yoon, M.J., Kim, J., Vierstra, R.D., and Chung, T. (2020). Arabidopsis cargo receptor NBR1 mediates selective autophagy of defective proteins. *J. Exp. Bot.* **71**: 73–89.
- Krissinel, E., and Henrick, K. (2007). Inference of macromolecular assemblies from crystalline state. *J. Mol. Biol.* **372**: 774–797.
- Kuromori, T., Fujita, M., Takahashi, F., Yamaguchi-Shinozaki, K., and Shinozaki, K. (2022). Inter-tissue and inter-organ signaling in drought stress response and phenotyping of drought tolerance. *Plant J.* **109**: 342–358.
- Lamark, T., Kirkin, V., Dikic, I., and Johansen, T. (2009). NBR1 and p62 as cargo receptors for selective autophagy of ubiquitinated targets. *Cell Cycle* **8**: 1986–1990.
- Lauwers, E., Erpapazoglou, Z., Haguenauer-Tsapis, R., and André, B. (2010). The ubiquitin code of yeast permease trafficking. *Trends Cell Biol.* **20**: 196–204.
- Li, X., Liu, Q., Feng, H., Deng, J., Zhang, R., Wen, J., Dong, J., and Wang, T. (2020). Dehydrin MtCAS31 promotes autophagic degradation under drought stress. *Autophagy* **16**: 862–877.
- Liu, L., Xiang, Y., Yan, J., Di, P., Li, J., Sun, X., Han, G., Ni, L., Jiang, M., Yuan, J., et al. (2021). BRASSINOSTEROID-SIGNALING KINASE 1 phosphorylating CALCIUM/CALMODULIN-DEPENDENT PROTEIN KINASE functions in drought tolerance in maize. *New Phytol.* **231**: 695–712.
- Luan, Q.L., Zhu, Y.X., Ma, S., Sun, Y., Liu, X.Y., Liu, M., Balint-Kurti, P. J., and Wang, G.F. (2021). Maize metacaspases modulate the defense response mediated by the NLR protein Rp1-D21 likely by affecting its subcellular localization. *Plant J.* **105**: 151–166.
- Mirdita, M., Schütze, K., Moriwaki, Y., Heo, L., Ovchinnikov, S., and Steinegger, M. (2022). ColabFold: Making protein folding accessible to all. *Nat. Methods* **19**: 679–682.
- Naranjo-Arcos, M., Srivastava, M., Deligne, F., Bhagat, P.K., Mansi, M., Sadanandom, A., and Vert, G. (2023). SUMO/deSUMOylation of the BRI1 brassinosteroid receptor modulates plant growth responses to temperature. *Proc. Nat. Acad. Sci. U.S.A.* **120**: e2217255120.
- Nie, S., Huang, S., Wang, S., Mao, Y., Liu, J., Ma, R., and Wang, X. (2019). Enhanced brassinosteroid signaling intensity via SIBRI1 overexpression negatively regulates drought resistance in a manner opposite of that via exogenous BR application in tomato. *Plant Physiol. Biochem.* **138**: 36–47.
- Paluch-Lubawa, E., Stolarska, E., and Sobieszczuk-Nowicka, E. (2021). Dark-induced barley leaf senescence—a crop system for studying senescence and autophagy mechanisms. *Front. Plant Sci.* **12**: 635619.
- Qi, H., Wang, Y., Bao, Y., Bassham, D.C., Chen, L., Chen, Q.F., Hou, S., Hwang, I., Huang, L., Lai, Z., et al. (2023). Studying plant autophagy: Challenges and recommended methodologies. *Adv. Biotechnol.* **1**: 2.
- Qi, H., Xia, F.N., and Xiao, S. (2021). Autophagy in plants: Physiological roles and post-translational regulation. *J. Integr. Plant Biol.* **63**: 161–179.
- She, J., Han, Z., Kim, T.W., Wang, J., Cheng, W., Chang, J., Shi, S., Wang, J., Yang, M., Wang, Z.Y., et al. (2011). Structural insight into brassinosteroid perception by BRI1. *Nature* **474**: 472–476.
- Siddiqui, M.N., Léon, J., Naz, A.A., and Ballvora, A. (2021). Genetics and genomics of root system variation in adaptation to drought stress in cereal crops. *J. Exp. Bot.* **72**: 1007–1019.
- Su, W., Bao, Y., Lu, Y., He, F., Wang, S., Wang, D., Yu, X., Yin, W., Xia, X., and Liu, C. (2021). Poplar autophagy receptor nbr1 enhances salt stress tolerance by regulating selective autophagy and antioxidant system. *Front. Plant Sci.* **11**: 568411.
- Sun, X., Wang, P., Jia, X., Huo, L., Che, R., and Ma, F. (2018). Improvement of drought tolerance by overexpressing MdATG18a is mediated by modified antioxidant system and activated autophagy in transgenic apple. *Plant Biotechnol. J.* **16**: 545–557.
- Suttangkakul, A., Li, F., Chung, T., and Vierstra, R.D. (2011). The ATG1/ATG13 protein kinase complex is both a regulator and a target of autophagic recycling in Arabidopsis. *Plant Cell* **23**: 3761–3779.
- Tarnowski, L., Rodriguez, M.C., Brzywczy, J., Piecho-Kabacik, M., Krčková, Z., Martinec, J., Wawrzynska, A., and Sirko, A. (2020). A selective autophagy cargo receptor NBR1 modulates abscisic acid signalling in *Arabidopsis thaliana*. *Sci. Rep.* **10**: 7778.
- Thirumalaikumar, V.P., Gorka, M., Schulz, K., Masclaux-Daubresse, C., Sampathkumar, A., Skirycz, A., Vierstra, R.D., and Balazadeh, S. (2021). Selective autophagy regulates heat stress memory in Arabidopsis by NBR1-mediated targeting of HSP90.1 and ROF1. *Autophagy* **17**: 2184–2199.
- Todaka, D., Shinozaki, K., and Yamaguchi-Shinozaki, K. (2015). Recent advances in the dissection of drought-stress regulatory networks and strategies for development of drought-tolerant transgenic rice plants. *Front. Plant Sci.* **6**: 84.

- Wang, H., Ding, Z., Gou, M., Hu, J., Wang, Y., Wang, L., Wang, Y., Di, T., Zhang, X., Hao, X., et al. (2021). Genome-wide identification, characterization, and expression analysis of tea plant autophagy-related genes (CsARGs) demonstrates that they play diverse roles during development and under abiotic stress. *BMC Genom.* **22**: 1–18.
- Wang, Q., Shen, T., Ni, L., Chen, C., Jiang, J., Cui, Z., Wang, S., Xu, F., Yan, R., and Jiang, M. (2023). Phosphorylation of OsRbohB by the protein kinase OsDMI3 promotes H<sub>2</sub>O<sub>2</sub> production to potentiate ABA responses in rice. *Mol. Plant* **16**: 882–902.
- Wang, Y., Cai, S., Yin, L., Shi, K., Xia, X., Zhou, Y., Yu, J., and Zhou, J. (2015). Tomato HsfA1a plays a critical role in plant drought tolerance by activating ATG genes and inducing autophagy. *Autophagy* **11**: 2033–2047.
- Wei, Y., Zeng, H., Liu, W., Cheng, X., Zhu, B., Guo, J., and Shi, H. (2021). Autophagy-related genes serve as heat shock protein 90 co-chaperones in disease resistance against cassava bacterial blight. *Plant J.* **107**: 925–937.
- Xiang, Y., Bian, X., Wei, T., Yan, J., Sun, X., Han, T., Dong, D., Zhang, G., Li, J., and Zhang, A. (2021b). ZmMPK5 phosphorylates ZmNAC49 to enhance oxidative stress tolerance in maize. *New Phytol.* **232**: 2400–2417.
- Xiang, Y., Sun, X., Bian, X., Wei, T., Han, T., Yan, J., and Zhang, A. (2021a). The transcription factor ZmNAC49 reduces stomatal density and improves drought tolerance in maize. *J. Exp. Bot.* **72**: 1399–1410.
- Yoo, C.Y., Pence, H.E., Jin, J.B., Miura, K., Gosney, M.J., Hasegawa, P. M., and Mickelbart, M.V. (2010). The Arabidopsis GTL1 transcription factor regulates water use efficiency and drought tolerance by modulating stomatal density via transrepression of SDD1. *Plant Cell* **22**: 4128–4141.
- Yu, P., and Hua, Z. (2022). The ubiquitin-26S proteasome system and autophagy relay proteome homeostasis regulation during silique development. *Plant J.* **111**: 1324–1339.
- Zhang, H., Zhu, J., Gong, Z., and Zhu, J.K. (2022a). Abiotic stress responses in plants. *Nat. Rev. Genet.* **23**: 104–119.
- Zhang, J., Wang, Y.Y., Pan, Z.Q., Li, Y., Sui, J., Du, L.L., and Ye, K. (2022b). Structural mechanism of protein recognition by the FW domain of autophagy receptor Nbr1. *Nat. Commun.* **13**: 3650.
- Zhang, Y., and Chen, Z. (2020). Broad and complex roles of NBR1-mediated selective autophagy in plant stress responses. *Cells* **9**: 2562.
- Zhao, P., Zhou, X.M., Zhao, L.L., Cheung, A.Y., and Sun, M.X. (2020). Autophagy-mediated compartmental cytoplasmic deletion is essential for tobacco pollen germination and male fertility. *Autophagy* **16**: 2180–2192.
- Zhou, J., Liu, D., Wang, P., Ma, X., Lin, W., Chen, S., Mishev, K., Lu, D., Kumar, R., Vanhoutte, S., et al. (2018). Regulation of Arabidopsis brassinosteroid receptor BRI1 endocytosis and degradation by plant U-box PUB12/PUB13-mediated ubiquitination. *Proc. Nat. Acad. Sci. U.S.A.* **115**: e1906–e1915.
- Zhou, J., Wang, J., Cheng, Y., Chi, Y.J., Fan, B., Yu, J.Q., and Chen, Z. (2013). NBR1-mediated selective autophagy targets insoluble ubiquitinated protein aggregates in plant stress responses. *PLoS Genet.* **9**: e1003196.
- Zientara-Rytter, K., Łukomska, J., Moniuszko, G., Gwozdecki, R., Surowiecki, P., Lewandowska, M., Liszewska, F., Wawrzyńska, A., and Sirko, A. (2011). Identification and functional analysis of Joka2, a tobacco member of the family of selective autophagy cargo receptors. *Autophagy* **7**: 1145–1158.

## SUPPORTING INFORMATION

Additional Supporting Information may be found online in the supporting information tab for this article: <http://onlinelibrary.wiley.com/doi/10.1111/jipb.13662/supinfo>

**Figure S1.** Pearson's correlation analysis between all biological replicate samples

**Figure S2.** Sequence alignment of NBR1 proteins from various plants

**Figure S3.** *ZmNBR1* expression in transgenic lines

**Figure S4.** Knockdown of *ZmNBR1* does not influence the expression of its homologous genes

**Figure S5.** Effects of *ZmNBR1* on stomatal closure and stomatal density

**Figure S6.** Interaction of *ZmNBR1* and its derivative proteins with different domains of *ZmBRI1a*

**Figure S7.** Expression of *ZmBRI1a* under drought stress

**Figure S8.** *ZmBRI1a* expression in transgenic lines

**Figure S9.** Knockdown of *ZmBRI1a* does not influence the expression of its homologous genes

**Figure S10.** Effects of *ZmBRI1a* on stomatal closure and stomatal density

**Figure S11.** *ZmBRI1a* forms a complex with *ZmNBR1* and *ZmATG8a*

**Figure S12.** The expression of *ZmNBR1* and *ZmBRI1a* in the RNA interference (RNAi)-*ZmNBR1*×RNAi-*ZmBRI1a* plants

**Figure S13.** Effect of *ZmNBR1* on the expression of the brassinosteroid (BR) pathway-related genes

**Figure S14.** Effect of *ZmBRI1a* on the expression of the autophagy-related genes

**Figure S15.** Effect of *ZmNBR1* and *ZmBRI1a* on the expression of the drought-related genes

**Figure S16.** Relative soil moisture during 8 d of drought stress

**Table S1.** Proteins, Interfaces, Structures and Assemblies (PISA) interface analysis of *ZmBRI1a* and *ZmNBR1* interaction bond forming residues

**Table S2.** Sequence information for primers used in this study



Scan using WeChat with your smartphone to view JIPB online



Scan with iPhone or iPad to view JIPB on Twitter